NASA CR 135320

Department of Aerospace Engineering
and Applied Mechanics
University of Cincinnati

ANALYSIS OF THE CROSS FLOW IN A RADIAL INFLOW TURBINE SCROLL

(NASA-CR-135320) ANALYSIS OF THE CROSS FLOW IN A RADIAL INFLOW TURBINE SCROLL (Cincinnati Univ.) 61 p HC A04/MF A01 CSCL 21E G3/07

N78-19153

Unclas 07350

BY

A. HAMED, S. ABDALLAH AND W. TABAKOFF

Supported by:

NATIONAL AERONAUTICS AND SPACE ADMINISTRATION

Lewis Research Center

Grant No. NSG 3066

NASA CR-135320

ANALYSIS OF THE CROSS FLOW IN A RADIAL INFLOW TURBINE SCROLL

by

A. Hamed, S. Abdallah and W. Tabakoff

Supported by:

NATIONAL AERONAUTICS AND SPACE ADMINISTRATION

Lewis Research Center

Grant No. NSG 3066

1. Report No	2 Government Accession No	3 Recipient's Catalog No
NASA CR 135320		

4 Title and Subtitle	5 Report Date
ANALYSIS OF THE CROSS FLOW IN A RADIAL INFLOW TURBINE SCROLL	November 1977
	6 Performing Organization Code

7. Author(s)	8 Performing Organization Report No
A. Hamed, S. Abdallah and W. Tabakoff	
	10 Work Unit No.

9 Performing Organization Name and Address	11 Contract or Grant No
Department of Aerospace Engineering & Applied Mechanics University of Cincinnati Cincinnati, Ohio 45221	NASA Grant NSG 3066
	13 Type of Report and Period Covered
12. Sponsoring Agency Name and Address	Contractor Report
National Aeronautical and Space Administration Washington, D.C. 20546	14 Sponsoring Agency Code

15 Supplementary Notes

16 Abstract

The equations of motion are derived, and a computational procedure is presented, for determining the nonviscous flow characteristics in the cross-sectional planes of a curved channel due to continuous mass discharge or mass addition. The analysis is applied to the radial inflow turbine scroll to study the effects of scroll geometry and the through flow velocity profile on the flow behavior. The computed flow velocity component in the scroll cross-sectional plane, together with the through flow velocity profile which can be determined in a separate analysis, provide a complete description of the three dimensional flow in the scroll.

17. Key Words (Suggested by Author(s))	18 Distribution Statement
Radial Machinery	Unclassified - unlimited

19 Security Classif (of this report)	20 Security Classif (of this page)	21 No of Pages	22 Price*
Unclassified	Unclassified	57	

* For sale by the National Technical Information Service Springfield Virginia 22161

TABLE OF CONTENTS

SUMMARY

The equations of motion are derived, and a computational procedure is presented, for determining the nonviscous flow characteristics in the cross-sectional planes of a curved channel due to continuous mass discharge or mass addition. The analysis is applied to the radial inflow turbine scroll to study the effects of scroll geometry and the through flow velocity profile on the flow behavior. The computed flow velocity component in the scroll cross-sectional plane, together with the through flow velocity profile which can be determined in a separate analysis, provide a complete description of the three dimensional flow in the scroll.

INTRODUCTION

Although radial turbines have been in operation for a very long time, there is a renewed interest in small radial inflow turbines. With advantages such as high efficiency over the limited range of specific speed, simplicity and ruggedness, these units are used in different applications such as automotive and diesel engines, aircraft cooling systems, and space power generation.

References [1], [2] and [3] are some examples of the recent interest in radial inflow turbine design and development. Several studies dealing with the prediction of the performance of these turbines can also be found in the literature [4-8]. While many flow studies were concerned with the flow in the impeller, very little has been done to investigate the flow in the rest of the turbine components. An experimental and theoretical study of the losses in the nozzle vanes and the vaneless nozzle is reported in Ref. [9]. It has been shown in that reference, that the performance of the vaned nozzle is greatly influenced by the flow incidence angle at inlet to the nozzle vanes. Therefore, in order to use any available loss analysis, the knowledge of the flow conditions at exit from the scroll is essential. A better understanding of the flow behavior in the scroll can thus contribute to a more accurate performance prediction.

The radial inflow turbine scroll is usually arranged in a helical configuration as shown in Fig. 1a to discharge uniformly into the nozzle of the radial turbine or the impeller in the case of nozzleless turbine. The actual flow in the scroll is three dimensional, compressible and viscous. Even in the absence of viscosity effects, the three dimensional flow is caused by the continuous flow discharge from the scroll. Although under real operating conditions other factors such as secondary flow effects may contribute to the three dimensional behavior of the flow, the effect of the radial component of the exit flux from the scroll will have the most predominant effect over the three dimensional flow behavior.

The present study investigates the three dimensional flow behavior in the scroll due to the continuous flow discharge. The equations governing the flow motion in the scroll are formulated in a special way in order to be solved in the cross sectional plane for a given through flow profile. Solutions are obtained numerically for the typical scroll cross sections of Figures 2 and 3, and the results are presented to show the effects of scroll geometry on the flow behavior in the scroll.

MATHEMATICAL FORMULATION

The differential equations governing the steady inviscid flow motion in the cross-sectional plane of the scroll will be developed. It is convenient for this purpose to consider the control volume, Ω, shown in Fig. 1b, which is contained between two cross-sectional planes.

The Equations of Motion:

Referring to the control volume of Fig. 1b, the equation of conservation of mass can be written as:

$$\iint_S \rho\, \bar{q}\cdot\bar{n}\, dS = 0 \qquad (1)$$

where ρ is the density, $\bar{q}$ is the flow velocity vector in the scroll, and $\bar{n}$ is the unit vector perpendicular to the surface, S, of the control volume. The surface, S, is the union of the scroll surface S_2, the cylindrical surface of the flow exit from the scroll S_1, and the two cross sectional planes A_1 and A_2.

On the two surfaces S_1 and S_2, $\bar{q}\cdot\bar{n}$ is equal to $\bar{V}\cdot\bar{n}$, where $\bar{V}$ is the velocity vector in the axial radial plane. Equation (1) can therefore be rewritten as:

$$\iint_{S_1+S_2} \rho\bar{V}\cdot\bar{n}\, dS = Q \qquad (2)$$

where Q is the net mass influx through the planes A_1 and A_2.

The difference between the mass flux on the surfaces A_1 and A_2 due to the through flow velocity can be represented by a continuous source distribution, g, in the control volume Ω according to the following relation:

$$Q = \iiint_{\Omega} g dv \tag{3}$$

Substituting equation (3) into equation (2) and using Gauss divergence theorem, we can write

$$\iiint_{\Omega} \text{div}(\rho \bar{V}) dv = \iiint_{\Omega} g dv \tag{4}$$

Since this equation is correct for any arbitrary control volume Ω of incremental depth, we can write:

$$\nabla \cdot (\rho \bar{V}) = g \tag{5}$$

For irrotational flow, the conservation of momentum is satisfied by introducing the velocity potential function ϕ, such that

$$\bar{V} = \nabla \phi \tag{6}$$

Substituting equation (6) into equation (5), we obtain the following relation

$$\nabla \cdot (\rho \nabla \phi) = g \tag{7}$$

The following isentropic relation is used to determine the density ρ, of the adiabatic, irrotational, nonviscous flow:

$$\rho = \rho_o \left(1 + \frac{\gamma-1}{2} \frac{q^2}{\gamma R_g T}\right)^{-\frac{1}{\gamma-1}} \tag{8}$$

where ρ_o is the flow stagnation density, and T is the flow temperature, which is a function of the stagnation temperature, T_o, and the magnitude of the flow velocity, q, according to the following relation:

$$T = T_o - \frac{(\gamma-1)q^2}{2\gamma R_g} \quad . \tag{9}$$

For given inlet stagnation conditions, equations (6) through (9) can be solved to determine the flow density, temperature and velocity components, in the cross sectional planes of a scroll. The solution will naturally depend on the source distribution which corresponds to the through flow profile at each cross section.

Equation (7) is rewritten in a different form, which will be used in the iterative numerical solution later.

$$\nabla^2\phi = -\frac{1}{\rho}\bar{V}\cdot\nabla\rho + g/\rho \tag{10}$$

It can be seen from this form that the velocity potential in the cross sectional plane is governed by Poisson's equation. The first term on the right hand side of equation (10) is a source or sink term contributed by the flow compressibility and the second term in the same equation represents the contribution of the through flow velocity to the source.

A very limited amount of experimental data is available from flow measurements in the scroll. Reference [8] reports only five points pressure measurements at one radial location in the scroll. On the other hand, the pressure measurements of Ref. [10] in the centrifugal pump, were obtained at the volute center. At the present time, detailed measurements through scroll cross sections are not available. Several factors such as the scroll radius of curvature, and the location of the particular cross section under consideration can affect the through flow velocity profile.

The condition of constant angular momentum has been applied to the flow in the scroll, and vaneless nozzles [3, 10]. In the absence of any blades to exert circumferential force on the flow, the product (ρwr) remains independent of the radial distance r, from the machine axis, where w is the through flow velocity. A variation in g, across the scroll cross section, that is proportional to 1/r, is one of the cases considered in the

results. For a given mass flow in the scroll, the proportionality constant will depend on the geometry of the cross section, and on the ratio of the particular cross sectional dimensions to the scroll radius of curvature at that section. A uniform, g, distribution is also considered, which corresponds to the case of a scroll with infinite radius of curvature, or a straight variable area tube with continuous uniform mass ejection. The boundary layer development will naturally cause variation from these profiles near the scroll walls, with the effects being more pronounced in the latter scroll sections. A third type of, g, distribution, namely that of a paraboloid of revolution in the circular part of the scroll cross section was also considered to study this viscous effect.

The Boundary Conditions

The equations governing the flow motion in the cross-sectional plane of the scroll, have been derived in the previous section. The boundary conditions will generally depend on the scroll geometry and the mass flow rate in the scroll.

Figures 2 and 3 show some typical scroll cross sectional geometries. Referring to these figures, the flow boundary conditions can be expressed as follows:

$$\bar{V}\cdot\bar{n} = V_1 \quad \text{on} \quad S_1 \tag{11}$$

$$\bar{V}\cdot\bar{n} = 0 \quad \text{on} \quad S_2 \tag{12}$$

where V_1 is the radial flow velocity at exit from the scroll. The boundary conditions given by equations (11) and (12) are of the Neumann type, when expressed in terms of the velocity potential function ϕ:

$$\frac{\partial\phi}{\partial n} = V_1 \quad \text{on} \quad S_1 \tag{13}$$

$$\frac{\partial\phi}{\partial n} = 0 \quad \text{on} \quad S_2 \tag{14}$$

Equations (13) and (14) provide the boundary conditions which are necessary to solve the governing equations (6), (8), (9) and (10). Two of the parameters appearing in these equations are not really independent. Both the source strength distribution, g, due to the through flow, and the outlet velocity, V_1, are related to the total mass flow rate in the scroll.

Assuming axisymmetric flow conditions at the scroll exit, and referring to Figures 2 and 3, we can write

$$\int_B \rho_1 V_1 \, ds = m/2\pi R_1 \tag{15}$$

where m is the rate of total mass flow in the scroll. The integral on the left hand side of equation (15) is carried over the scroll exit width, B, of radial location, R_1, of which the density and velocity are equal to ρ_1 and V_1 respectively.

The mean value of g, can also be expressed in terms of the total mass flow rate, m, as follows:

$$\iint_A g \, dA = m/2\pi R_1 \tag{16}$$

where the integral on the left hand side is carried over the scroll cross sectional area. Equations (15) and (16) can be combined to give the following relation:

$$\iint_A g \, dA = \int_B \rho_1 V_1 \, dS \tag{17}$$

It is well known that a solution to Poisson equation with Neumann boundary conditions exists and is unique within an arbitrary constant if Green's first integral theorem is satisfied. Closer examination of equations (10) and (13) show that in the special case of incompressible flow, equation (17) represents Green's first integral condition.

NONDIMENSIONAL FORM OF THE GOVERNING EQUATIONS

It is more convenient to express the flow variables in the following dimensionless form:

$$\phi^* = \phi/V_1 D \quad , \quad \bar{V}^* = \bar{V}/V_1 \quad ,$$

$$T^* = T/T_o \quad , \quad \rho^* = \rho/\rho_o \quad , \tag{18}$$

$$g^* = \frac{D}{\rho_o V_1} g \quad .$$

where D is a characteristic dimension of the scroll cross-section, which can be taken as the diameter in the typical sections of Figures 2 and 3. The coordinates are also normalized with respect to D. In the above equations and in the following derivations, the radial exit velocity component, V_1, will be taken as constant across the scroll exit width, B. Using equation (18), one can write the flow governing equations in nondimensional form as follows:

Equations of Motion:

$$\nabla^{*2}\phi^* = -\frac{1}{\rho^*}(\bar{V}^* \cdot \nabla^* \rho^*) + g^*/\rho^* \tag{19}$$

$$\bar{V}^* = \nabla^* \phi^* \tag{20}$$

$$T^* = 1 - C_k q^{*2} \tag{21}$$

$$\rho^* = (1 + C_k q^{*2}/T^*)^{-\frac{1}{\gamma-1}} \tag{22}$$

Boundary Conditions:

$$\frac{\partial \phi^*}{\partial n^*} = 1 \quad \text{on} \quad S_1 \tag{23}$$

$$\frac{\partial \phi^*}{\partial n^*} = 0 \quad \text{on} \quad S_2 \tag{24}$$

where

$$C_k = \frac{(\gamma-1)\ V_1^2}{\gamma R_g T_o} \tag{25}$$

Equations (23) and (24) show that the boundary conditions of the nondimensional problem are homogeneous, thus leading to self similar solutions in the case of geometrically similar scroll cross sections with similar through flow profiles.

The above equations are not tractable to analytical solutions in scroll cross sections such as the typical ones shown in Figures 2 and 3. A numerical solution which is based on the finite difference method is used to determine the two dimensional velocity potential distribution on the scroll cross-sectional plane. Before writing the governing equations in finite difference form, equations (19), (20), (23) and (24) are rewritten using the Cartesian coordinates as follows:

$$\frac{\partial^2 \phi^*}{\partial x^{*2}} + \frac{\partial^2 \phi^*}{\partial y^{*2}} = -\frac{1}{\rho^*}\left(u^* \frac{\partial \rho^*}{\partial x^*} + v^* \frac{\partial \rho^*}{\partial y^*}\right) + g^*/\rho^* \tag{26}$$

$$u^* = \frac{\partial \phi^*}{\partial x^*} \quad \text{and} \quad v^* = \frac{\partial \phi^*}{\partial y^*} \tag{27}$$

$$\frac{\partial \phi^*}{\partial x^*} = 1 \qquad \text{on} \quad S_1 \tag{28}$$

$$n_x \frac{\partial \phi^*}{\partial x^*} + n_y \frac{\partial \phi^*}{\partial y^*} = 0 \quad \text{on} \quad S_2 \tag{29}$$

where u^*, v^* are the x and y components of the nondimensional velocity vector in the cross-sectional plane, and n_x, n_y are the direction cosines of the unit vector which is perpendicular to S_2. According to equation (28), the two perpendicular axes will be taken such that y is in the direction of the machine axis.

NUMERICAL SOLUTION

The derivations of the finite difference equations is followed by a description of the iterative procedure used to obtain the numerical solution.

The Finite Difference Equations:

Referring to Figure 4, the finite difference representation of equation (26) is obtained using standard five-point Laplace difference operator.

$$\phi_o^* = [\delta_{13}(\phi_{11}^*+\phi_{33}^*)+ BB\delta_{24}(\phi_{22}^*+\phi_{44}^*)- \frac{F^*}{2} Dx^2]/(C_{13}+C_{24}) \quad (30)$$

where

$$BB = (Dx/Dy)^2 \quad ,$$

$$C_{13} = 1/\delta_1\delta_3 \quad , \quad C_{24} = BB/\delta_2\delta_4 \quad , \quad (31)$$

$$\delta_{13} = 1/(\delta_1+\delta_3) \quad , \quad \delta_{24} = 1/(\delta_2+\delta_4) \ .$$

$$\phi_{ii}^* = \phi_i^*/\delta_i \quad , \quad i = 1, 2, 3, 4 \quad (32)$$

$$F^* = g^*/\rho^* - \frac{1}{\rho^*}\left(u^* \frac{\partial \rho^*}{\partial x^*} + v^* \frac{\partial \rho^*}{\partial y^*}\right) \quad (33)$$

The first order derivatives needed in the u^* and v^* calculations, as well as the derivatives of the density in equation (33), are evaluated using central difference formulas at the interior points. Forward or backward difference schemes were used in the first order derivative computations at the boundaries of the scroll cross section. The boundary conditions can generally be written in the following form:

$$n_x \frac{\partial \phi^*}{\partial x^*} + n_y \frac{\partial \phi^*}{\partial y^*} = L \quad (34)$$

where n_x and n_y are the direction cosines of the normal to the boundary, and L is a constant which is equal to one or zero as in equations (28) and (29).

Referring to Fig. 5, and for a general boundary point, 4, one can write the boundary condition in the following finite difference form [11]:

$$\phi_4^* = \left(1 + \frac{n_x}{n_y}\,\delta_4\,\frac{Dy}{Dx}\right)\phi_o^* - \frac{n_x}{n_y}\,\delta_4\,\frac{Dy}{Dx}\,\phi_3^* - \frac{\delta_4 Dy}{n_y}\,L \qquad (35)$$

Similar equations can be written for the boundary points on the other three quarters by proper permutation. The solution to equations (30) and (35) is obtained using a successive relaxation iterative method which is explained later. In the following sections, the superscript star will be omitted for convenience, when referring to the nondimensional variables.

Interdependence Between the Source Distribution and the Boundary Conditions:

It is well known that in the case of Poisson equation with Neumann boundary conditions, a solution exists, and is unique within an arbitrary constant, if the following condition is satisfied:

$$\iint_A F(x,y)\,dA = \int_s \frac{\partial \phi}{\partial n}\,ds \qquad (36)$$

where F(x,y) is the source strength in Poisson equation, which is equal to the sum of two terms on the right hand side of equation (10). The integrals in the above equation are carried over the solution domain, A, and its boundary, s, respectively.

In case the source distribution F(x,y) in the differential equation is arbitrarily chosen, the above condition will not necessarily be satisfied. This was the case in Ref. [15], in which Briley, before proceeding with the numerical solution of Poisson equation, added a uniform correction to the source distribution. He accomplished that by computing numerically, the difference E, between the right hand and left hand sides of equation (36), then subtracting the area averaged amount, E/A,

from the value of F(x,y), at each grid point. In the case of incompressible flow, such procedure is unnecessary since the source strength, F, is equal to g, which already satisfies the conservation of mass, given by the integral condition of equation (17). For compressible flow solution, in which case, F(x,y) is also dependent on the velocity and density at the grid points, the average value of the difference between the two sides of equation (36) is calculated numerically and subtracted from the value of F at each interior grid point before every iteration.

ITERATIVE PROCEDURE

A successive relaxation method is used to obtain the numerical solution. The following recurrence formula is used:

$$\phi_o^{n+1} = (1-\omega)\phi_o^n + \omega(\delta_{13}[\phi_{11}^{n+1} + \phi_{33}^n] + BB\ \delta_{24}[\phi_{22}^n + \phi_{44}^{n+1}] - \frac{F}{2} Dx^2)/(C_{13} + C_{24}) \quad (37)$$

The computations of the contribution of the compressibility to the source term were allowed to lag the potential function calculations by one iteration. Taking the value of the density from the previous iteration is known to improve the stability of the numerical solution to compressible flow problems [12].

Boundary Conditions in the Iterative Scheme:

The general recurrence formula for the iterative solution is given by equation (37). If this is used to determine the value of ϕ at all interior points, and equations similar to (35) are to calculate explicitly the boundary values of ϕ, the solution will not converge but will drift slowly and endlessly [15, 16]. Miyakoda [16] therefore recommended that the boundary conditions be implicitly introduced into the difference equations at the interior points next to the boundary such as point O in Fig. 5. Referring to the same figure, the following form of finite difference equation is used at the interior points adjacent to the boundary:

$$\phi_o^{n+1} = (1-\omega)\phi_o^n + \omega(\delta_{13}[\phi_{11}^{n+1} + \phi_{33}^n] + BB\ \delta_{24}[\phi_{22}^n + (\frac{1}{\delta_4} + \frac{n_x}{n_y}\frac{Dy}{Dx})\phi_o^{n+1} - \frac{n_x}{n_y}\frac{Dy}{Dx}\phi_3^n - \frac{Dy}{n_y}L] - \frac{F}{2}Dx^2)/(C_{13}+C_{24}) \quad (38)$$

Similar expressions can be written for such points in the other three quarters of the domain. These equations are solved algebraically for ϕ_o^{n+1}, appearing in both sides. The solutions to the difference equations consisting of equation (37) at the regular interior points and equation (38), at the interior points adjacent to the boundary, was found to converge. The numerical values of the potential function at the interior grid points calculated in this fashion are then used in difference equations (35) to compute the values of ϕ at the boundary points.

Choice of Under-Relaxation Factor:

The convergence of the numerical solution to Poisson equation is known to be sensitive to the relaxation factor. In the matrix solution to compressible flow equation in turbomachines using the relaxation methods, the under-relaxation is known to get stronger as the Mach number approaches unity. The boundary conditions in those problems are different however from those involved in the present study. In addition to Dirichlet type at parts of the domain boundary, they include periodicity and specified flow angles over the rest of the boundary. Furthermore, solutions to the Reynolds equation which is similar to equation (7), were also easily obtained using relaxation methods in both lubrication problems [13], and magnetostatic fields [14], when Dirichlet type boundary conditions were involved. In such cases an optimum value of the under-relaxation factor can be used at all grid points. In the present solution an optimum value was determined by trial and error and was used in equation (37) at all the regular interior points that are removed at least one grid point from the boundary. The same value of, ω, was not necessarily used

in equation (38) at the interior grid points adjacent to the boundary. When necessary, other values of ω were chosen in order that the following condition is satisfied:

$$[1 - \omega BB\ \delta_{24}\ (\frac{1}{\delta_4} + \frac{n_x}{n_y}\frac{Dy}{Dx})/(C_{13} + C_{24})] \neq 0 \quad . \tag{39}$$

RESULTS AND DISCUSSION

A computer program has been developed to solve the governing flow equations in the cross-sectional planes of the scroll of arbitrary cross section. The input to the program consists of the fluid properties at the scroll inlet, the exit radial velocity, the scroll geometric dimensions and the through flow velocity profile. The typical geometric parameters needed in the input are shown in Figures 2 and 3 for the symmetric and nonsymmetric scroll cross sections. The maximum number of allowable mesh points is (50 x 30), in the x and y directions, respectively. In all the results presented here the computation time did not exceed 30 CPU seconds.

The results of the computations are presented in the form of plots of constant potential contours, and arrows showing the velocity directions in the scroll cross sectional plane. The effects of through flow velocity profile, scroll cross sectional geometry, and compressibility on the flow behavior in the cross sectional plane are investigated.

Figures 6 and 7 were obtained using uniform source distribution, representing uniform through flow velocity profile. The results obtained using a source variation which is proportional to y_r are presented in Figures 8 through 11 to show the effects of the scroll curvature. Figures 12 and 13 present the results in the case of a circular paraboloid source distribution. All the results of Figures 6 through 13 were computed for a scroll with symmetric scroll cross section, in which case it was sufficient to carry out the computations in only half the cross section. Zero potential gradient was specified in this case

at the axis of symmetry. The results obtained from computations in a scroll with an unsymmetric cross section are shown in Figures 14 and 15. The compressible flow results, which were obtained at an exit Mach number of 0.7, are presented in Figures 16 and 17. All the last four figures were obtained with a uniform source distribution, i.e., excluding the influence of the scroll's curvature. In all the figures, higher velocity potential gradients are observed at the exit portion of the scroll cross sections. This means velocity components in the cross sectional plane are higher in magnitude in this region than in the rest of the scroll cross sections. Since the solution for the velocity potential is unique within an arbitrary constant, the value of 0.1 was always chosen at the neck of the cross section in order to compare the different results.

Figures 6 and 7 show in the case of symmetric scroll cross section with constant through flow velocity profile, that nowhere in the flow field does the velocity have component in the radially outward direction. The largest radial velocity components are observed at the scroll exit portion, decreasing constantly to zero value at the radially farthest scroll surface point on the axis of symmetry.

Figures 8 through 11 show the velocity potential distribution and the velocity direction in the case of a source distribution which is inversely proportional to r. The first two figures correspond to a ratio of the scroll's radius of curvature to cross sectional diameter of 3.0 while the last two figures show the results for R/D of 1.5. The influence of the scroll's curvature on the flow behavior can be detected by comparing Figs. 9 and 11 with 7; and 10 and 12 with 8. It can be seen that the influence of the curvature is limited to the radially outward part of the cross section, leading to a difference in the direction of the velocity vector in the cross sectional plane. Some radially outward velocities can be observed in Figs. 9 and 12, although the magnitudes of the

velocity in this region are very small. The ratios of R/D in Figs. 8 through 11 are quite low however, and were merely selected for the purpose of illustration. Such magnitudes would not be encountered in radial inflow turbine scrolls, where the value of R/D constantly increases from its minimum value at the scroll inlet. It can therefore be concluded that in most scroll cross sections it is sufficient to consider constant source distribution in the cross sectional computations.

Figures 12 and 13 show the results obtained using a circular paraboloid source distribution, which represents an extreme case corresponding to fully developed pipe flow. It can be seen from these figures that some radially outward velocity components, even though of very small values, are observed at radially outer portion of the scroll cross section. In this case, the magnitude of the velocity component in the cross section plane, as measured by the velocity potential gradient, is generally smaller in most of the scroll cross sections, compared to the case of constant source distribution. It should be pointed out, that in all the cases of Figures 8 through 13, the values of the integral of the source distribution over the scroll cross section were all the same and equal to the value for the case of constant source distribution of Figures 6 and 7.

The velocity potential contours and the velocity directions of the velocity vector in a nonsymmetric scroll cross section are shown in Figures 14 and 15. These results were obtained using uniform through flow profile. It can be seen that the flow behavior is generally smoother in this case, which can be a result of the more gradual change in the scroll section in the direction of the machine axis. This type of scroll cross section, can therefore be recommended over the symmetric section.

The compressible flow solution corresponding to an exit Mach number of 0.7 is shown in Figures 16 and 17. These results, in a symmetric scroll cross section, were calculated assuming

constant through flow velocity profile. By comparing these two figures with the incompressible results of Figures 6 and 7, it can be concluded that the shape of the velocity potential contours is unaffected by compressibility. Consequently, the shape of the streamlines is not changed by compressibility, although the magnitudes of the velocities are. While higher velocities are observed in the scroll neck region, lower velocities are found in the rest of the scroll cross sectional plane as compared to the incompressible case.

CONCLUSION

The known through flow velocity, which is used to provide the source distribution, and the computed flow velocity in the cross sectional plane provide a complete description of the three dimensional flow field in the scroll. A derivation of the equations governing the flow motion and a computational procedure for determining the flow velocities in the cross-sectional plane are presented in this study. Other simplified flow models can be used in the through flow velocity computations.

REFERENCES

1. Calvert, G.S. and Okapuu, U., "Design and Evaluation of a High Temperature Radial Turbine," Phase I - Final Report, USAAVLABS Technical Report 68-69.
2. Watanabe, I., Ariga, I. and Mashimo, T., "Effect of Dimensional Parameters of Impellers on Performance Characteristics of a Radial Inflow Turbine," ASME Paper No. 70-GT-90.
3. Lagneau, J.P., "Contribution to the Study of Advanced Small Radial Gas Turbines," VKI IN 38, March 1970.
4. Kastner, L.J. and Bhinder, F.S., "A Method for Predicting the Performance of a Centripetal Gas Turbine Fitted With A Nozzle-Less Volute Casing," ASME Paper No. 75-GT-65.
5. Wallace, F.J., Cave, P.R. and Miles, J., "Performance of Inward Radial Flow Turbines Under Steady Flow Conditions With Special Reference to High Pressure Ratios and Partial Admission," Proc. Instn. Mech. Engrs., Vol. 184, Pt. 1, No. 56, 1969-1970.
6. Samuel, M.F., and Wasserbauer, C.A., "Off-Design Performance Prediction With Experimental Verification for a Radial Inflow Turbine," NASA TND 2621, 1965.
7. Knoernschild, E.M., "The Radial Turbine for Low Specific Speeds and Low Velocity Factors," Journal of Engineering for Power, Trans. ASME, Series A, Vol. 83, No. 1, January 1961, pp. 1-8.
8. Watanabe, I. and Ando, T., "Experimental Study on Radial Turbine With Special Reference to the Influence of the Number of Impeller Blades on Performance Characteristics," Bulletin of JSME, Vol. 2, No. 7, 1959, pp. 457-462.
9. Khalil, I.M., Tabakoff, W. and Hamed, A., "Losses in Radial Inflow Turbines," Journal of Fluids Engineering, September 1976, pp. 364-373.
10. Iversen, H.W., Rolling, R.E. and Carlson, J.J., "Volute Pressure Distribution, Radial Force on the Impeller, and Volute Mixing Losses of a Radial Flow Centrifugal Pump," Journal of Engineering for Power, April 1960, pp. 136-144.

11. Parker, R., "Short Communications Normal Gradient Boundary Conditions in Finite Difference Calculations," International Journal for Numerical Methods in Engineering, Vol. 7, No. 3, 1974, pp. 397-400.
12. Smith, D.J.L. and Frost, D.H., "Calculation of the Flow Past Turbomachine Blades," Proceedings of the Institute of Mechanical Engineers, Vol. 184, Part 36 (II), 1969-1970.
13. Holmes, A.G. and Ettles, C.M.M., "A Study of Iterative Solution Techniques for Elliptic Partial Differential Equations With Particular Reference to the Reynolds Equation," Computer Methods in Applied Mechanics and Engineering, Vol. 5, 1975, pp. 309-328.
14. Winslow, A., "Numerical Solution to the Quasilinear Poisson Equation in a Nonuniform Triangle Mesh," Journal of Computational Physics, Vol. 2, 1967, pp. 149-172.
15. Briley, W.R., "Numerical Method for Predicting Three-Dimensional Steady Viscous Flow in Ducts," Journal of Computational Physics, Vol. 14, 1974, pp. 1-20.
16. Miyakoda, K., "Contribution to the Numerical Weather Prediction Computation with Finite Difference," Japanese Journal of Jeophysics, Vol. 3, 1962, pp. 160-167.

NOMENCLATURE

C_k	Nondimensional expression defined in equation (25).
B	Scroll exit width, Figs. 2 and 3.
BB, C_{13}, C_{24}	Expressions defined in equation (31).
D_o	Scroll inlet diameter, Figure 1.
D,H	Characteristic dimensions of the scroll cross-section, Figs. 2 and 3.
F	Expression defined in equation (33).
g	Source strength distribution in the scroll cross-section, due to the through flow.
L	A constant equal to one or zero on the boundary, equation (34).
m	Total rate of mass flow in the scroll.
$\bar{n}$	Local unit vector normal to the scroll surface.
n_x, n_y	Components of the unit vector $\bar{n}$, in the x and y directions, respectively.
$\bar{q}$	Velocity vector in the scroll.
Q	Difference in rate of mass flow across two radial planes, equation (2).
R_1	Radius of the scroll exit, Fig. 1.
R_g	Gas constant.
S	Surface of the control volume Ω, Figure 1.
s	Distance along the boundary contour of the scroll cross section.
T	Local static gas temperature.
T_o	Stagnation temperature.
u,v	Velocity components in the scroll cross sectional plane in the x and y directions, respectively.
$\bar{V}$	Velocity vector in the axial radial plane.
V_1	Velocity component in the radial direction at the scroll exit.

Greek Symbols

ϕ	The velocity potential function in the cross-sectional plane.
ρ	Local gas density.
ρ_o	Stagnation density.
ρ_1	Flow static density at the scroll exit.
δ	Mesh size parameter, Fig. 4.
δ_{13}, δ_{24}	Expressions defined in equation (31).
ω	Successive relaxation factor.
Ω	The control volume of Fig. 1.

Subscripts

i=1,2,3&4	Refer to parameters associated with the five mesh points of Fig. 4.
x,y	Refer to derivatives in the x and y directions.

Superscripts

*	Refer to the nondimensional variables.
n,n+1	Refer to the previous and present iterations.

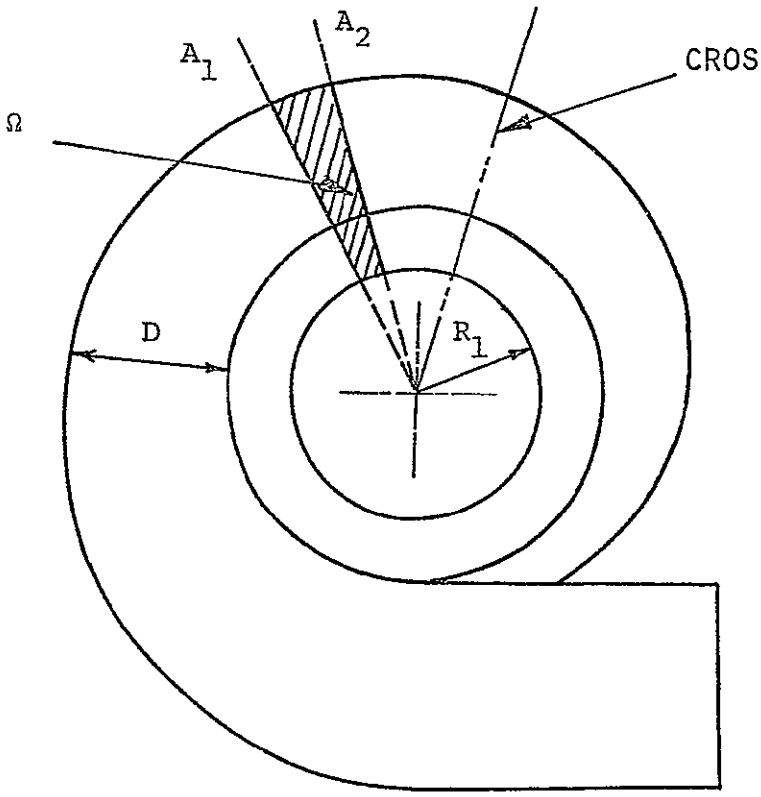

FIG. 1A

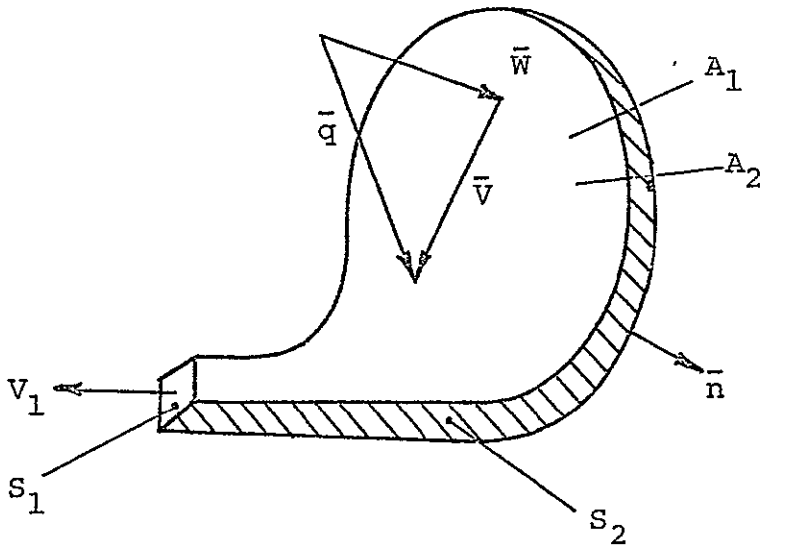

FIG. 1B. CONTROL VOLUME Ω

FIG. 1. RADIAL INFLOW TURBINE SCROLL

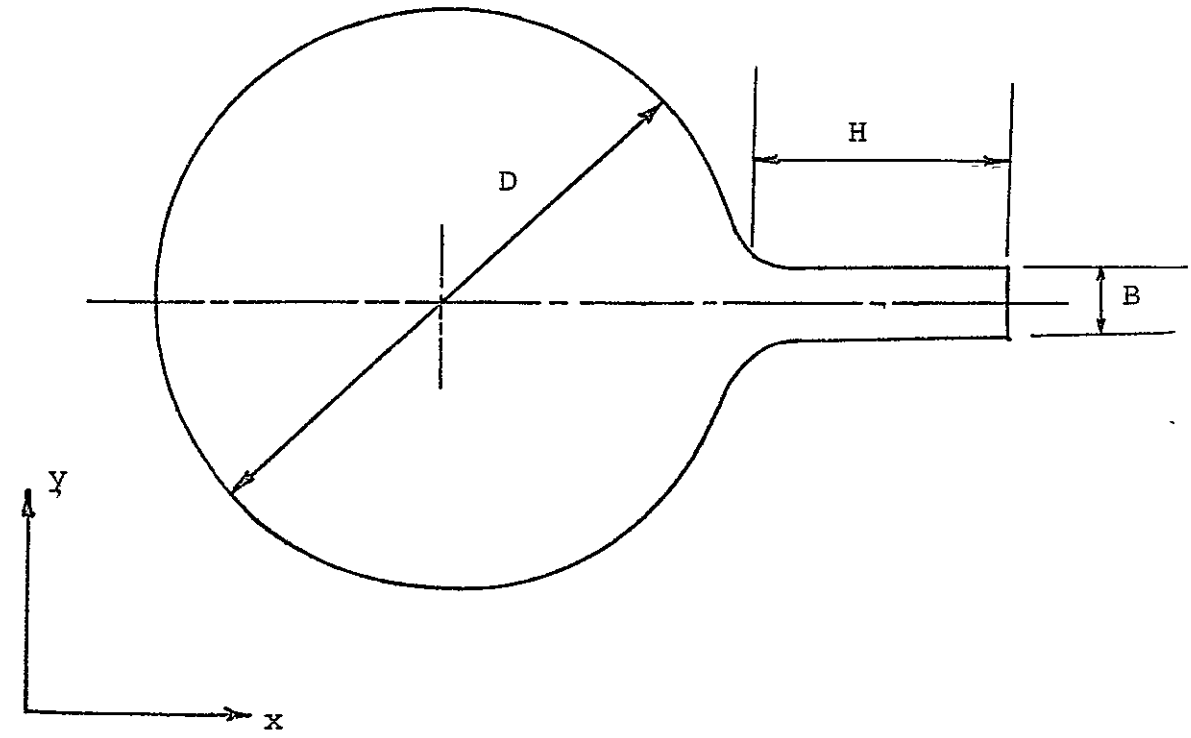

FIG. 2. SYMMETRIC SCROLL CROSS SECTION

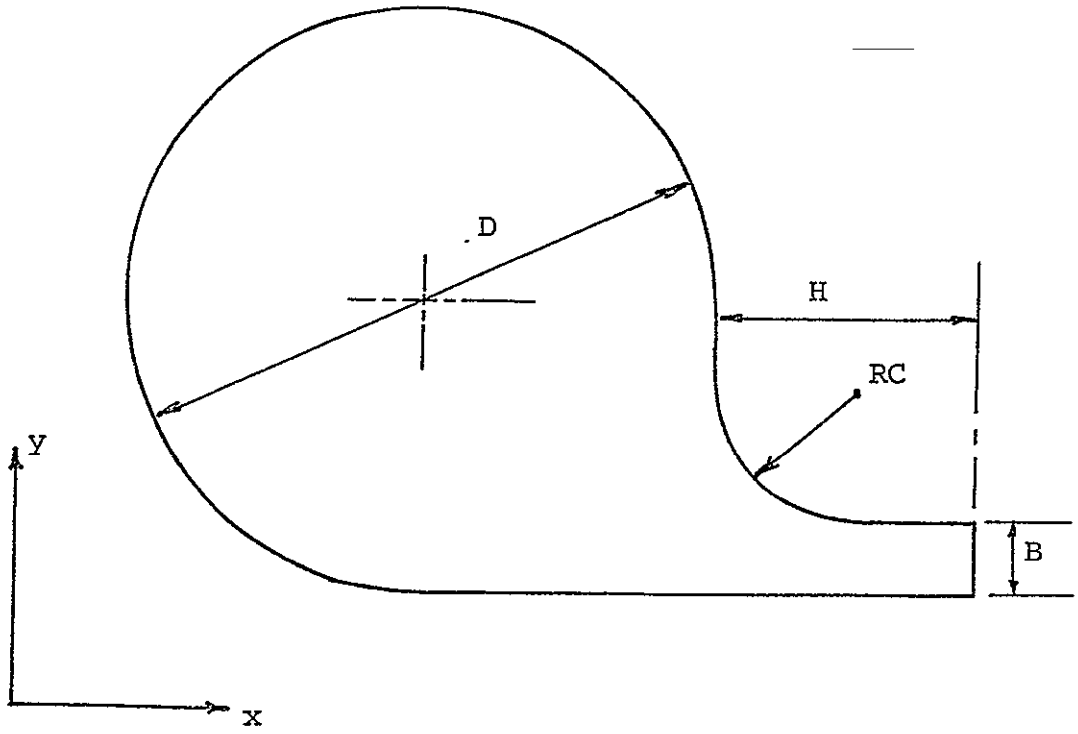

FIG. 3. NON SYMMETRIC SCROLL CROSS SECTION.

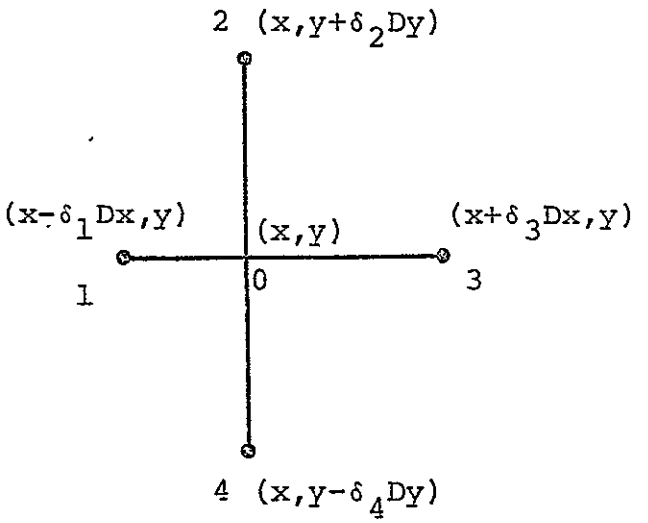

FIG. 4. GRID POINTS IN THE FINITE DIFFERENCE SCHEME.

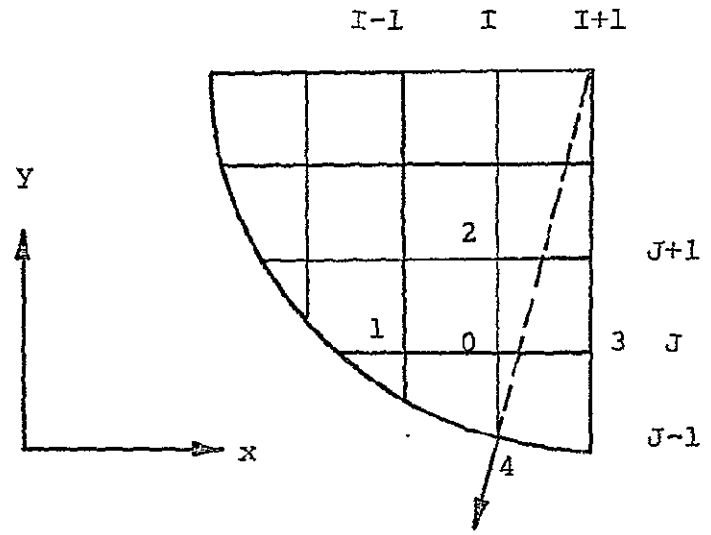

FIG. 5. GRID SYSTEM FOR INTERIOR POINTS.

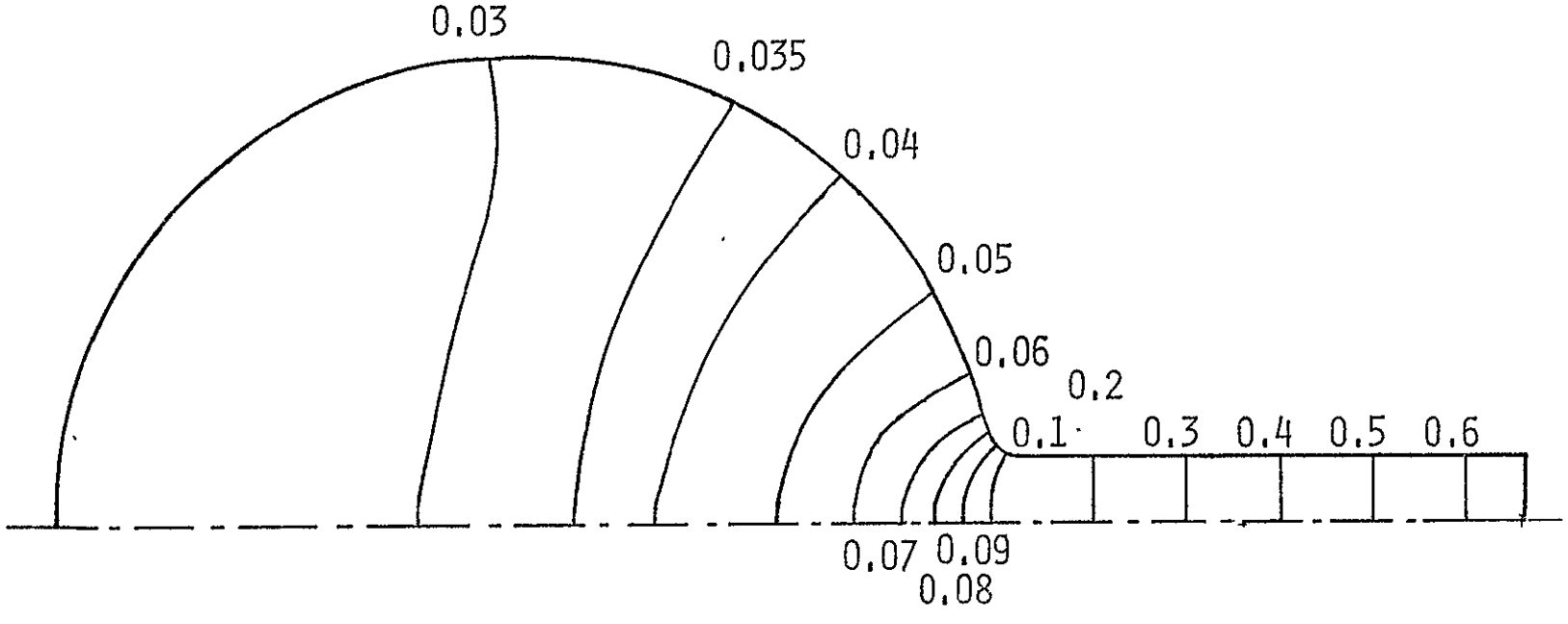

FIG. 6. NON-DIMENSIONAL VELOCITY POTENTIAL DISTRIBUTION IN A SYMMETRIC SCROLL CROSS SECTION FOR UNIFORM THROUGH FLOW VELOCITY PROFILE.

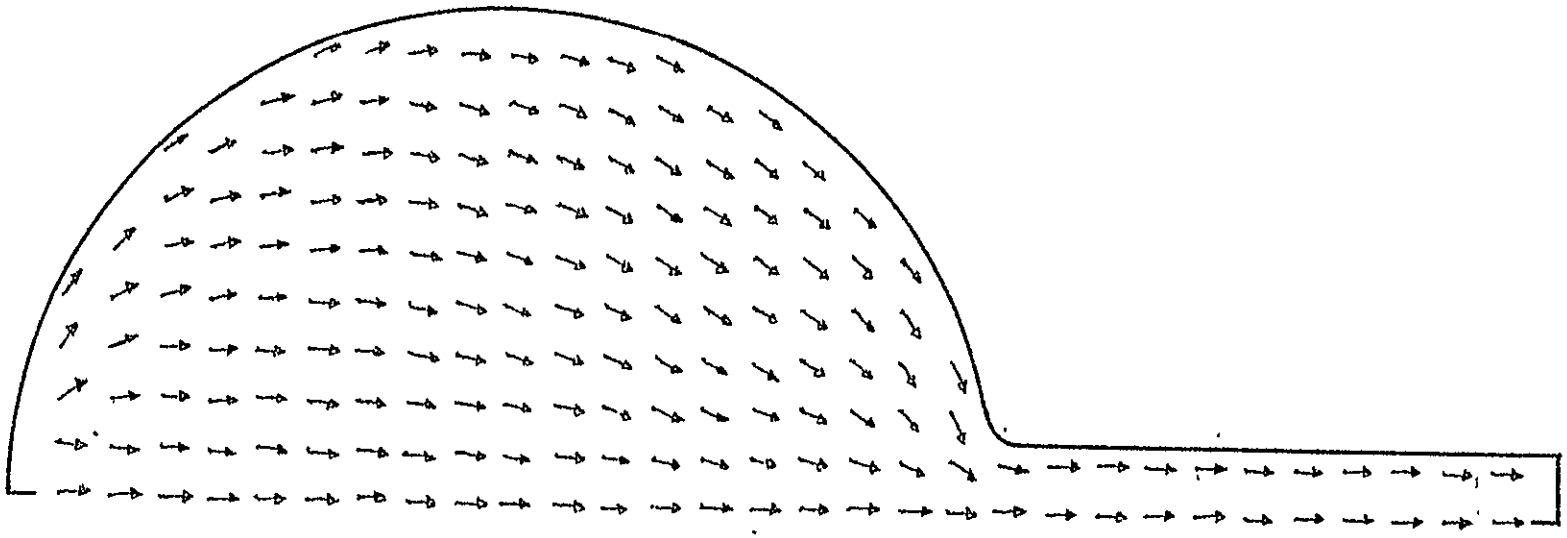

FIG. 7. THE DIRECTION OF THE VELOCITY VECTOR IN THE CROSS-SECTIONAL PLANE OF A SYMMETRIC SCROLL FOR UNIFORM THROUGH FLOW VELOCITY

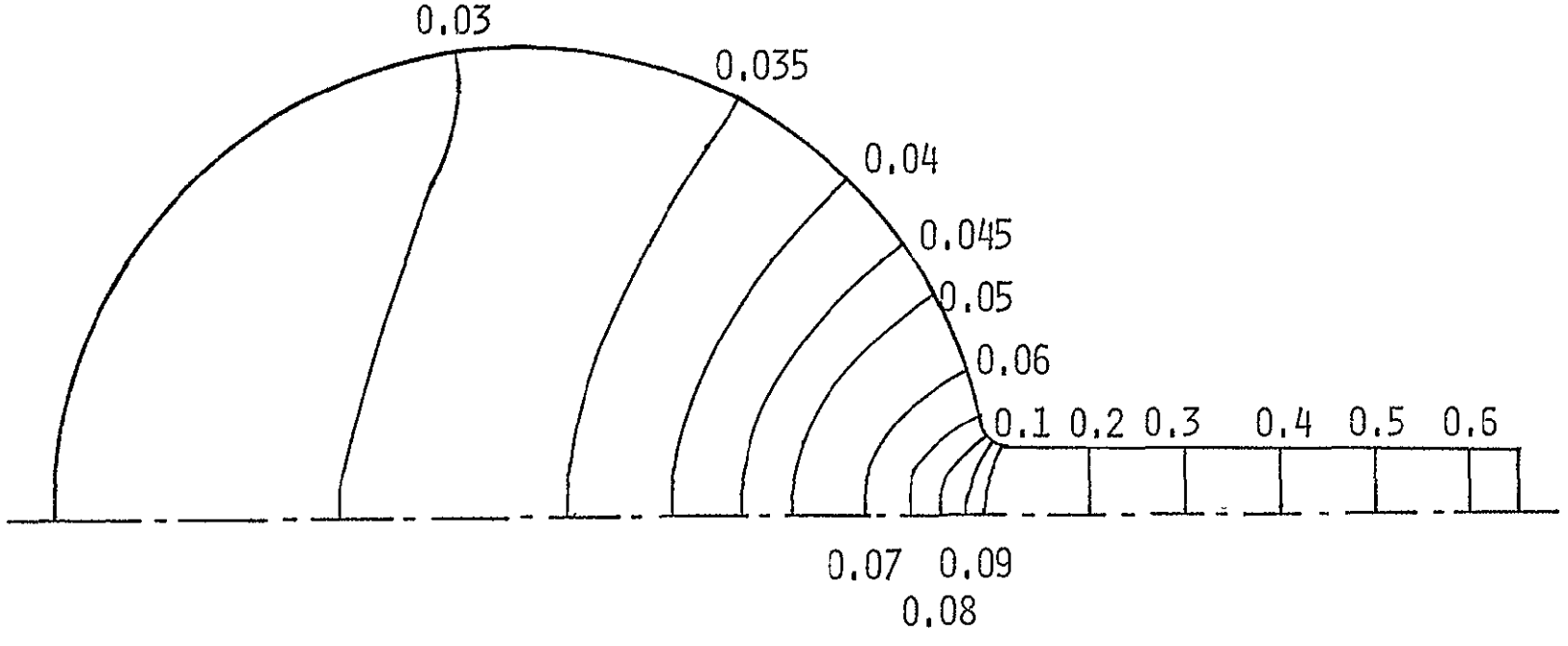

FIG. 8. NON-DIMENSIONAL VELOCITY POTENTIAL CONTOURS SHOWING THE EFFECT OF SCROLL CURVATURE (R/D = 3).

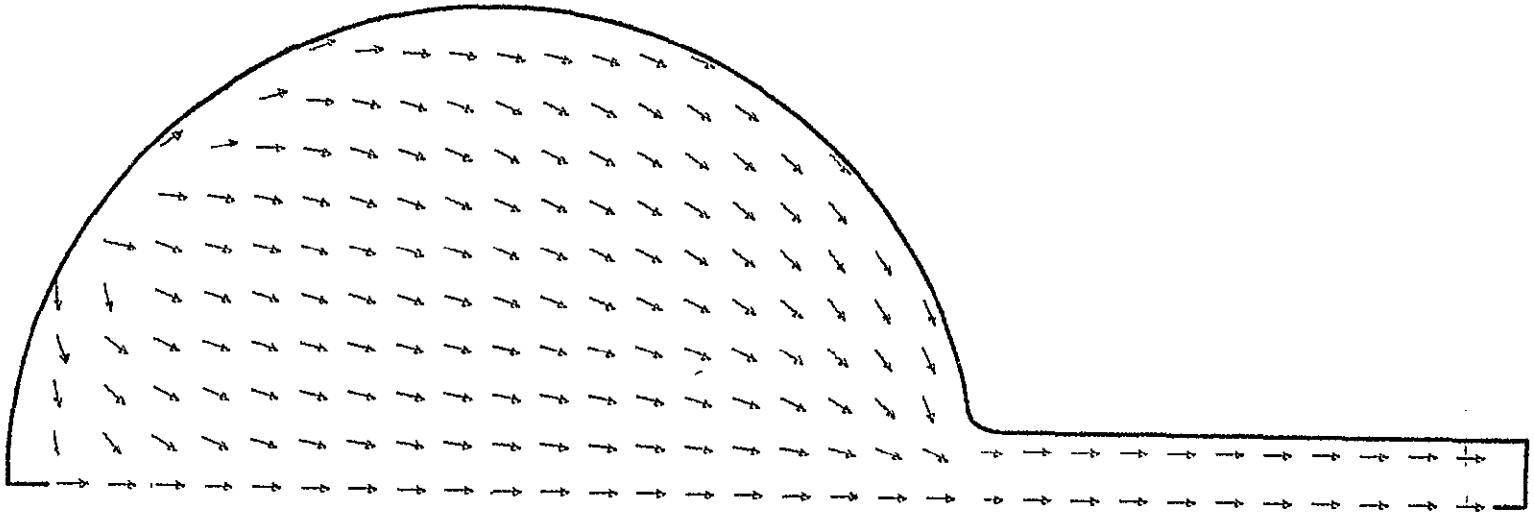

FIG. 9. THE DIRECTION OF THE VELOCITY VECTOR IN THE CROSS SECTION PLANE SHOWING THE EFFECT OF SCROLL CURVATURE (R/D = 3).

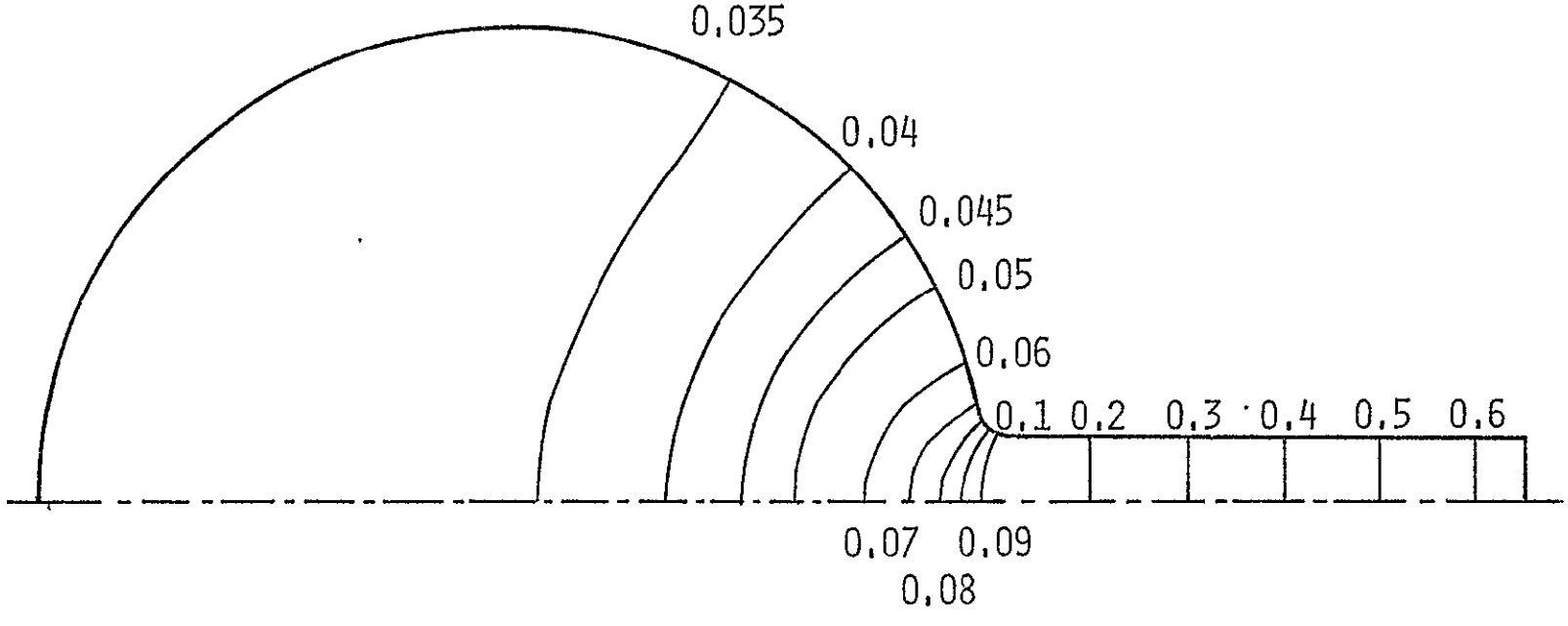

FIG. 10. NON-DIMENSIONAL VELOCITY POTENTIAL CONTOURS SHOWING THE EFFECT OF SCROLL CURVATURE (R/D = 1.5).

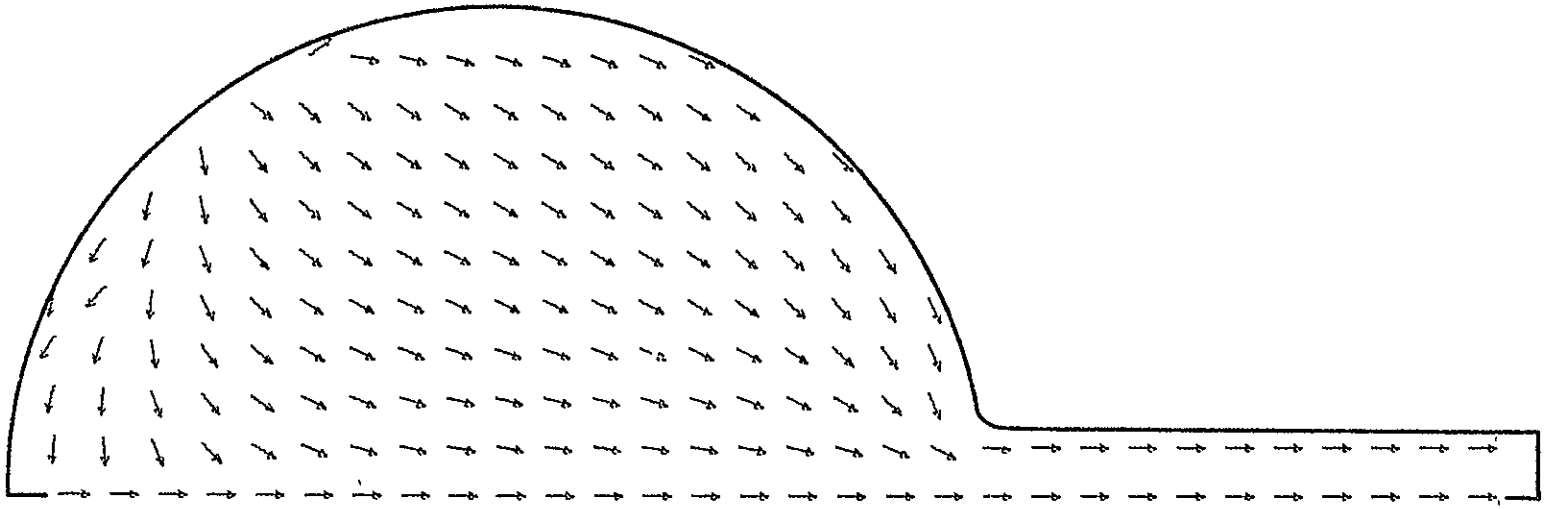

FIG. 11. THE DIRECTION OF THE VELOCITY VECTOR IN THE CROSS SECTION PLANE SHOWING THE EFFECT OF SCROLL CURVATURE (R/D = 1.5).

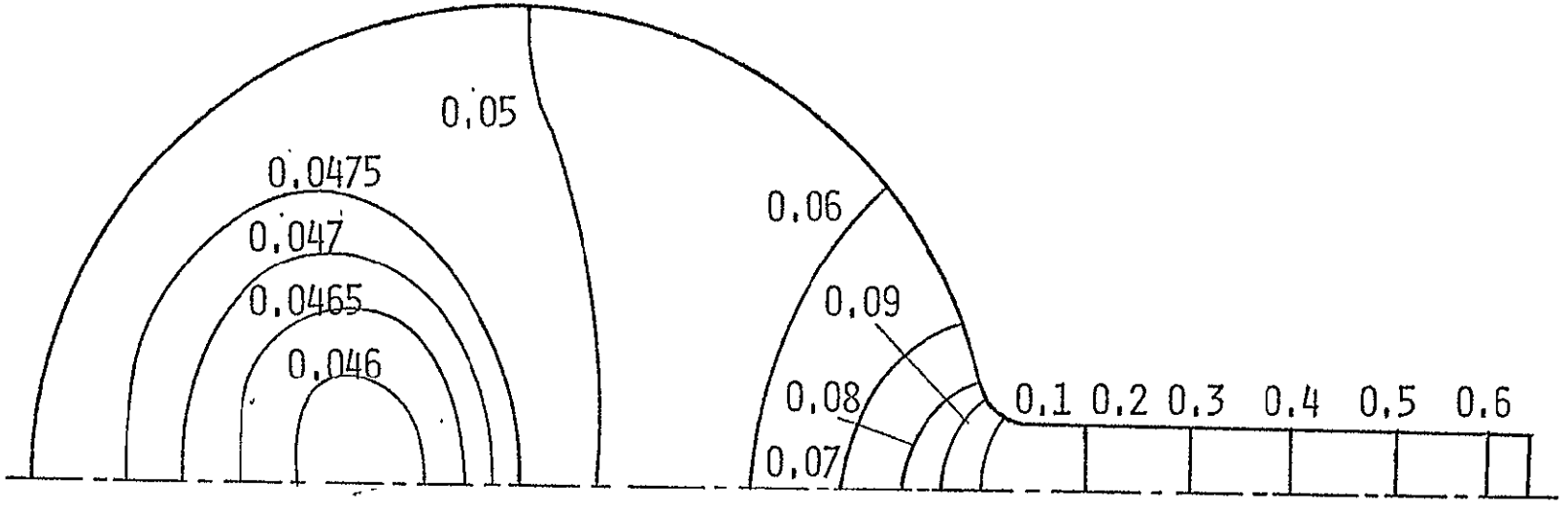

FIG. 12. NON-DIMENSIONAL VELOCITY POTENTIAL DISTRIBUTION IN A SYMMETRIC SCROLL CROSS SECTION FOR CIRCULAR PARABOLOID THROUGH FLOW VELOCITY PROFILE

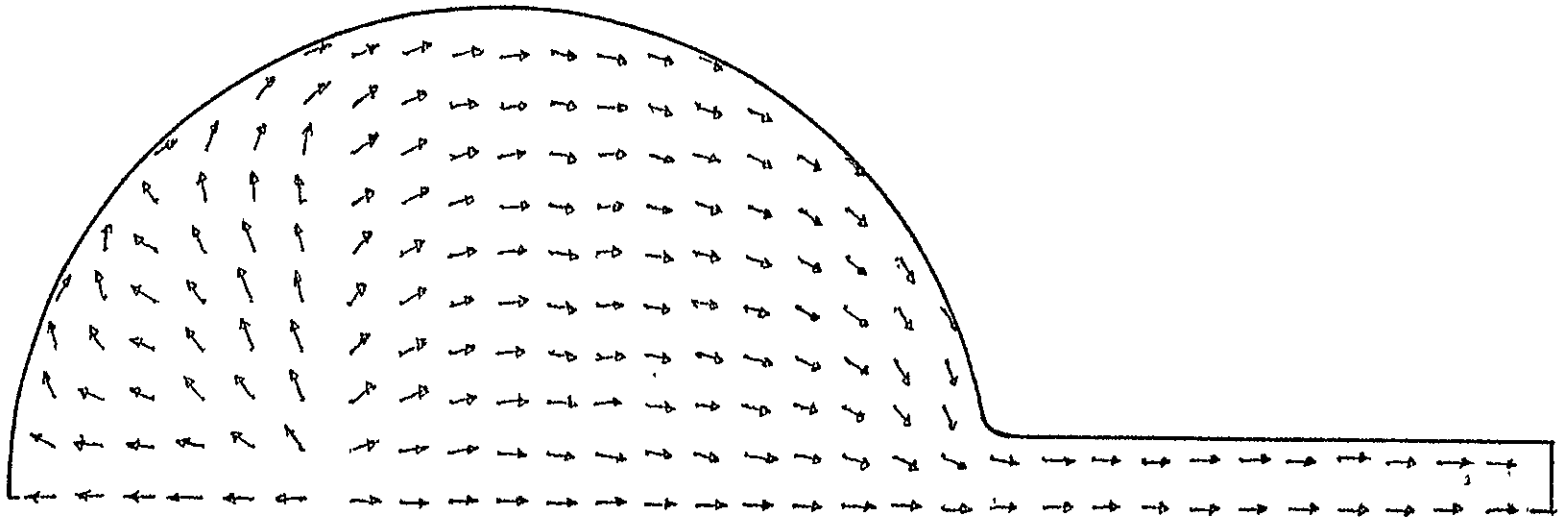

FIG. 13. THE DIRECTION OF THE VELOCITY VECTOR IN THE CROSS-SECTION PLANE OF A SYMMETRIC SCROLL CROSS SECTION FOR CIRCULAR PARABOLOID THROUGH FLOW VELOCITY PROFILE

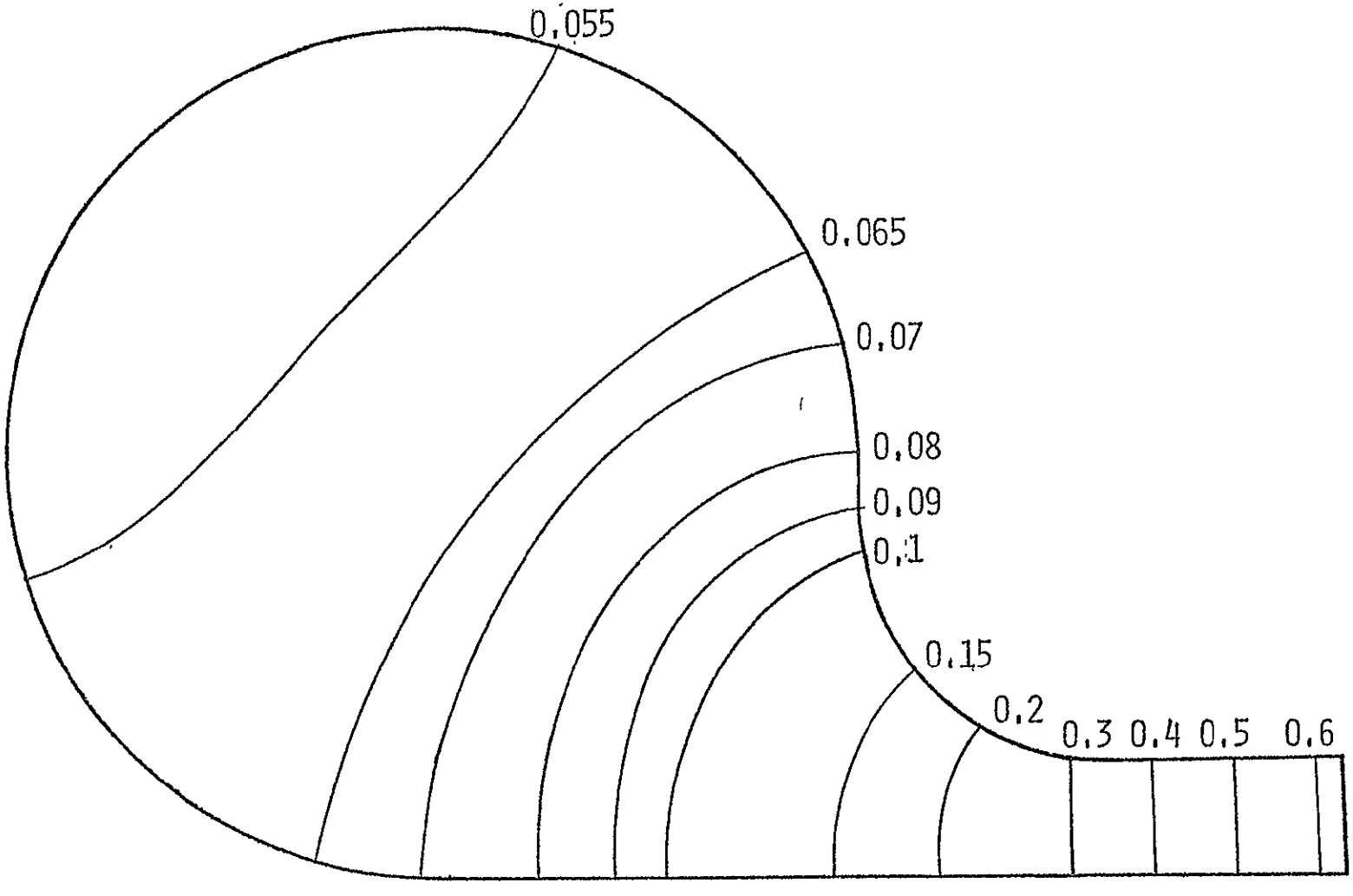

FIG. 14. NON-DIMENSIONAL VELOCITY POTENTIAL DISTRIBUTION IN A NON-SYMMETRIC SCROLL CROSS SECTION FOR UNIFORM THROUGH FLOW VELOCITY PROFILE

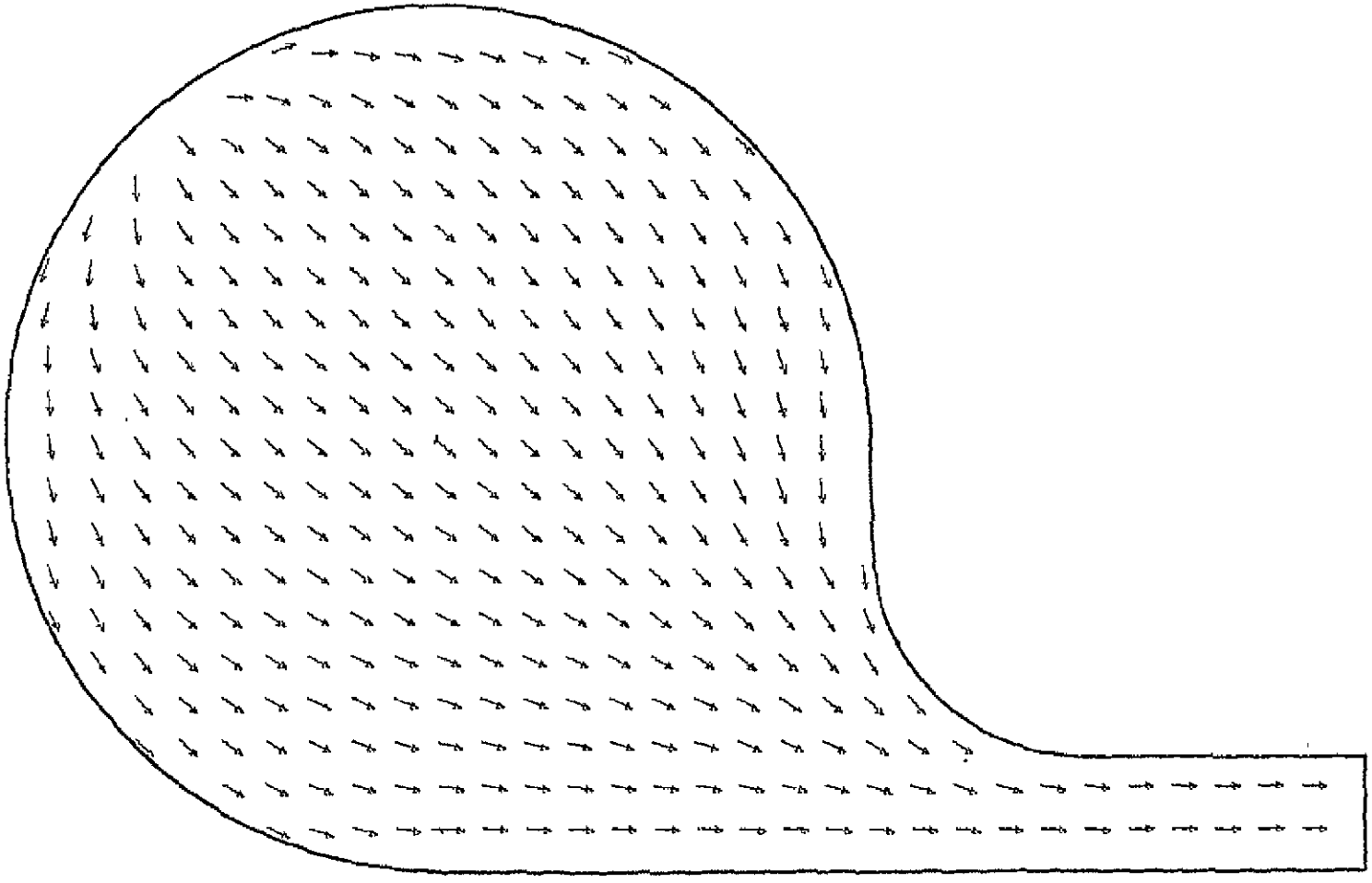

FIG. 15. THE DIRECTION OF THE VELOCITY VECTOR IN THE CROSS-SECTIONAL PLANE OF A NON SYMMETRIC SCROLL FOR UNIFORM THROUGH FLOW VELOCITY PROFILE.

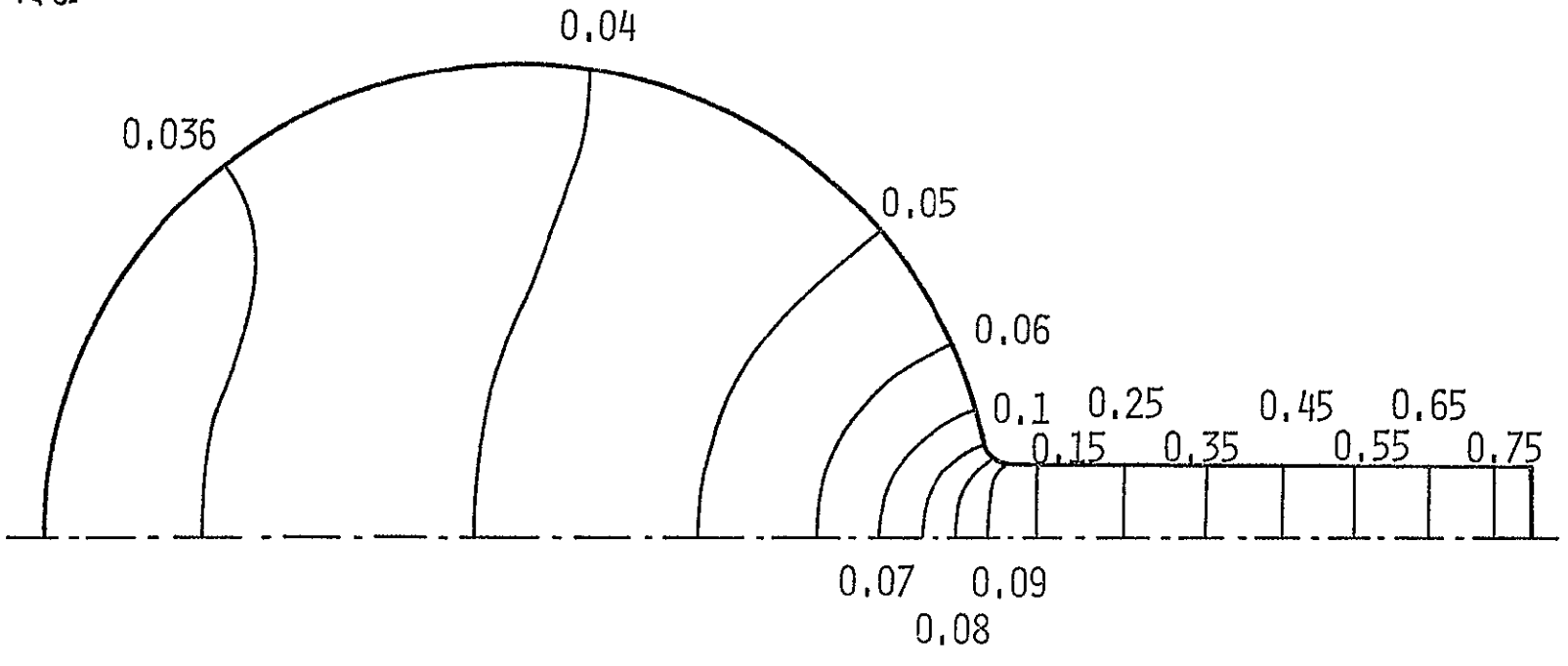

FIG. 16. NON-DIMENSIONAL VELOCITY POTENTIAL DISTRIBUTION OF COMPRESSIBLE FLOW IN A SYMMETRIC SCROLL CROSS SECTION FOR UNIFORM THROUGH FLOW VELOCITY PROFILE.

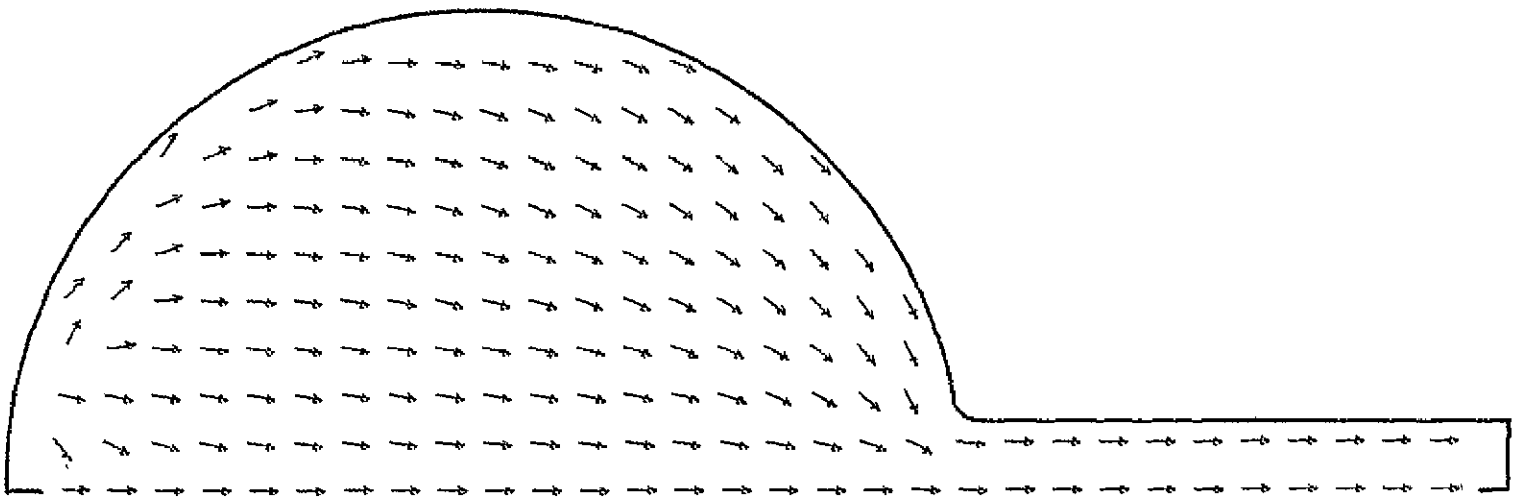

FIG. 17. THE DIRECTION OF THE COMPRESSIBLE FLOW VELOCITY VECTOR IN THE CROSS SECTION PLANE OF A SYMMETRIC SCROLL CROSS SECTION FOR UNIFORM THROUGH FLOW VELOCITY PROFILE.

APPENDIX

COMPUTER PROGRAM AND INPUT PREPARATION

A brief description of the input and output of the computer program will be given in this appendix. A listing of the program, which can be used to solve the equations of potential flow in the cross-sectional planes of radial inflow turbine can be obtained from

Description of Input and Output

The computer program requires as input the cross sectional plane geometry, the radius of curvature at the plane, appropriate shape of the through flow profile, and the operating conditions such as the inlet velocity and the inlet total temperature. Any consistant set of units can be used in the input data. The computations are carried out and the results presented in terms of the dimensionless quantities given in equation (18).

The output obtained from the program includes cross-sectional plane velocities and potential velocity values throughout the region of solution.

Input Data

First Set (Fluid Properties), one card

READ: RG, GAMA, TO, VE

according to format (4F10.0)

RG	Gas constant.
GAMA	Ratio of specific heats.
TO	Stagnation temperature.
VE	Scroll exit velocity in radial direction.

Second Set (Scroll Geometry), one card

READ: M1, M2, DO, R1, B, H, R, RC

according to format (2I10, 6F10.0)

M1, M2	Number of mesh lines in the circular part of the cross-section of the scroll in the x and y directions, respectively (Figure 3a).
DO	Scroll inlet diameter.

R1 — Scroll radius of curvature, Fig. 1a.

B — Width of the scroll exit, Figs. 2 and 3.

H — Length of scroll exit nozzle, Figs. 2 and 3.

R — Radius of the scroll cross-section equal D/2, Figs. 2 and 3.

RC — Radius of exit portion of the unsymmetric cross-section, Fig. 3.

Third Set (Control Parameters), one card

READ: ICOM, ISYM, IFG, IPAP, IFREVO

according to format (5I10)

ICOM — Parameter to control type of calculations. ICOM = 0 for incompressible flow and ICOM = 1 for compressible flow.

ISYM — Parameter to control type of scroll cross section. For symmetric cross-section ISYM = 1, and for unsymmetric cross section ISYM = 0.

IFG, IPAP, IFREVO — Parameters to control the mass source distribution (i.e., the type of through flow velocity profile).

(i) IFG = 1, IPAP = 0, IFREVO = 0, for an arbitrary source distribution. In this case the value of the mass source is fed as input at all the interior mesh points.

(ii) IPAP = 1, IFG = 0, IFREVO = 0, for a circular paraboloid source distribution.

(iii) IFREVO = 1, IPAP = 0, IFG = 0, for free vortex source distribution

(iv) IFG = 0, IPAP = 0, IFREVO = 0, represents the uniform source distribution.

Fourth Set (Numerical Parameters), one card

READ: ITMAX, EPSMAX, WO, WOP

according to format (I10, 3F10.0)

ITMAX — Maximum allowable number of iterations.

EPSMAX — The largest tolerable value of the square of the sum of the absolute values of the deviations of $\phi_{i,j}$ from their previously computed values.

WO, WOP — Successive relaxation factors, for interior mesh points, and for the points adjacent to the boundaries, respectively.

Fifth Set (Output Control Parameters), one card

READ: IP, IVPLOT, IPLT

according to format (3I10)

IP	Frequence of intermediate printout. Solutions are printed after every IP iterations.
IVPLOT	Parameter to control plotting of program output, IVPLOT = 1, a plot is prepared; if IVPLOT = 0, no plot is prepared.
IPLT	Number of contours in the output plot for the potential velocity.

Sixth Set (Values for Velocity Potential Contour Plotting), number of cards is equal to IPLT

READ: VISOBR

according to format (F10.0)

VISOBR	Numerical values of the velocity potential contours to be plotted as output.

Seventh Set (Arbitrary Source Distribution)

Is required only in the case of arbitrary source distribution, i.e., IFG = 1. The value of the source distribution F(I,J) is read in DO loop according to format (8F10.0). The input data is fed starting from I = 1 to I = M_3, and marching in J direction from J = JL, JU as shown in figure 1A.

Output

The program output includes a printout of the pertinent flow properties at all the grid points every IP iterations and of two figures one for the desired velocity potential contours as specified by IPLT and VISOBR and the second showing the velocity direction in the cross-sectional plane.

Explanation of the labels of the print output are given below:

F	Vector containing the values of Poisson's source strength at each grid point.
P	Vector containing the values of the potential function ϕ at all grid points.

PBX, PBY	Vectors containing the values of ϕ on the scroll boundaries.
VV	Vector containing the absolute values of the velocity vector $\bar{V}$, at each grid point.
VVBX, VVBY	Vectors containing the absolute values of the velocity vector $\bar{V}$, at the boundary points for each I and J mesh lines, respectively.
THETA	Vector containing the values of the angle between the velocity vector $\bar{V}$, and the x-axis at each grid point.

DATA OF THE SCROLL CROSS SECTION

```
GAS CONSTANT = 287.40000
GAMA         =   1.40000
STAG. TEMP.  = 300.00000
RAD. EXIT VEL= 200.00000

M1   =        21
M2   =        11
D0   =  12.70000
R1   =   1.90426
B    =   0.07447
H    =   0.59574
RC   =   0.0
D    =   9.40000  UNIT DIM.

ICOM =         0
ISYM =         1
IFG  =         0
IPAP =         0
IFREVO=        0

ITMAX=       250
LPSMAX=0.000000001
WO   =   0.95000
WOP  =   0.95000

IP   =       400
IVPLOT=        1
IPLT =        20

     DX   =   0.05000     DY   =   0.05000     IC   =        11     JC   =         1
M1   =        32     N3   =         2
```

POISSONS SOURCE DIS. AT EACH GRID POINT

```
  I  =        2
0.2198905  0.2198905  0.2198905  0.2198905  0.2193905  0.0        0.0        0.0        0.0        0.0

  I  =        3
0.2198905  0.2198905  0.2198905  0.2198905  0.2198905  0.2198905  0.0        0.0        0.0        0.0

  I  =        4
0.2198905  0.2198905  0.2198905  0.2198905  0.2198905  0.2198905  0.2198905  0.2198905  0.0        0.0
```

I = 5
0.2198905 0.2198905 0.2198905 0.2198905 0.2198905 0.2198905 0.2198905 0.2198905 0.0 0.0

I = 6
0.2198905 0.2198905 0.2198905 0.2198905 0.2198905 0.2198905 0.2198905 0.2198905 0.2198905 0.0

I = 7
0.2198905 0.2198905 0.2198905 0.2198905 0.2198905 0.2198905 0.2198905 0.2198905 0.2198905 0.2198905

I = 8
0.2198905 0.2198905 0.2198905 0.2198905 0.2198905 0.2198905 0.2198905 0.2198905 0.2198905 0.2198905

I = 9
0.2198905 0.2198905 0.2198905 0.2198905 0.2198905 0.2198905 0.2198905 0.2198905 0.2198905 0.2198905

I = 10
0.2198905 0.2198905 0.2198905 0.2198905 0.2198905 0.2198905 0.2198905 0.2198905 0.2198905 0.2198905

I = 11
0.2198905 0.2198905 0.2198905 0.2198905 0.2198905 0.2198905 0.2198905 0.2198905 0.2198905 0.2198905

I = 12
0.2198905 0.2198905 0.2198905 0.2198905 0.2198905 0.2198905 0.2198905 0.2198905 0.2198905 0.2198905

I = 13
0.2198905 0.2198905 0.2198905 0.2198905 0.2198905 0.2198905 0.2198905 0.2198905 0.2198905 0.2198905

I = 14
0.2198905 0.2198905 0.2198905 0.2198905 0.2198905 0.2198905 0.2198905 0.2198905 0.2198905 0.2198905

I = 15
0.2198905 0.2198905 0.2198905 0.2198905 0.2198905 0.2198905 0.2198905 0.2198905 0.2198905 0.2198905

I = 16
0.2198905 0.2198905 0.2198905 0.2198905 0.2198905 0.2198905 0.2198905 0.2198905 0.2198905 0.0

I = 17
0.2198905 0.2198905 0.2198905 0.2198905 0.2198905 0.2198905 0.2198905 0.2198905 0.0 0.0

ORIGINAL PAGE IS
OF POOR QUALITY

I = 18									
0.2198905	0.2198905	0.2198905	0.2198905	0.2198905	0.2198905	0.2198905	0.2198905	0.0	0.0
I = 19									
0.2198905	0.2198905	0.2198905	0.2198905	0.2198905	0.2198905	0.0	0.0	0.0	0.0
I = 20									
0.2198905	0.2198905	0.2198905	0.2198905	0.2198905	0.0	0.0	0.0	0.0	0.0
I = 21									
0.2198905	0.2198905	0.0	0.0	0.0	0.0	0.0	0.0	0.0	0.0
I = 22									
-0.0007556	-0.0007556	0.0	0.0	0.0	0.0	0.0	0.0	0.0	0.0
I = 23									
-0.0007556	-0.0007556	0.0	0.0	0.0	0.0	0.0	0.0	0.0	0.0
I = 24									
-0.0007556	-0.0007556	0.0	0.0	0.0	0.0	0.0	0.0	0.0	0.0
I = 25									
-0.0007556	-0.0007556	0.0	0.0	0.0	0.0	0.0	0.0	0.0	0.0
I = 26									
-0.0007556	-0.0007556	0.0	0.0	0.0	0.0	0.0	0.0	0.0	0.0
I = 27									
-0.0007556	-0.0007556	0.0	0.0	0.0	0.0	0.0	0.0	0.0	0.0
I = 28									
-0.0007556	-0.0007556	0.0	0.0	0.0	0.0	0.0	0.0	0.0	0.0
I = 29									
-0.0007556	-0.0007556	0.0	0.0	0.0	0.0	0.0	0.0	0.0	0.0
I = 30									
-0.0007556	-0.0007556	0.0	0.0	0.0	0.0	0.0	0.0	0.0	0.0

```
   I  =        31
-0.0007556  -0.0007556   0.0          0.0          0.0          0.0          0.0          0.0          0.0          0.0

   I  =        32
-0.0007556  -0.0007556   0.0          0.0          0.0          0.0          0.0          0.0          0.0          0.0
```

********** **********

EPS = 0.67370-05
NO. OF ITERATIONS= 250

********** **********

VALUES OF POTENTIAL VELOCITY P(I,J) FOR INCOMPRESSIBLE FLOW

```
J = 1
  0.0                -0.9630153940-01   -0.5644747570-01   -0.9632138040-01   -0.5610009090-01   -0.5579285170-01
 -0.5535992470-01    -0.5479140260-01   -0.5405609400-01   -0.5315021630-01   -0.5203966030-01   -0.5065741260-01
 -0.4896947190-01    -0.4688802920-01   -0.4433743240-01   -0.4112740350-01   -0.3700724360-01   -0.3151324340-01
 -0.2173055320-01    -0.1173601260-01    0.0924214000-02    0.4804958500-01    0.9083333770-01    0.1346030930 00
  0.1789331230 00     0.2238206580 00    0.2693197110 00    0.3155609780 00    0.3625679310 00    0.4103931130 00
  0.4590768070 00     0.5088364440 00

J = 2
  0.0                -0.9657105850-01   -0.5652180860-01   -0.5640429520-01   -0.5619542360-01   -0.5588423610-01
 -0.5548549670-01    -0.5409182350-01   -0.5417261250-01   -0.5347207110-01   -0.5216107540-01   -0.5079991320-01
 -0.4913679440-01    -0.4710424290-01   -0.4460752500-01   -0.4150885230-01   -0.3759702290-01   -0.3254869540-01
 -0.2560578970-01    -0.1584312940-01    0.0                0.4035190490-01    0.9056634350-01    0.1346402320 00
  0.1790518050 00     0.2239765510 00    0.2695211750 00    0.3157686790 00    0.3627854050 00    0.4106221210 00
  0.4593127440 00     0.5088747010 00

J = 3
  0.0                -0.9658800430-01   -0.5656131140-01   -0.5643731080-01   -0.5620207070-01   -0.5590554050-01
 -0.5551171310-01    -0.5500540050-01   -0.5430791990-01   -0.5343626860- 01  -0.5236291910-01   -0.5105399250-01
 -0.4946714770-01    -0.4754992270-01   -0.4523216020-01   -0.4243029030-01   -0.3904131690-01   -0.3497037320-01
 -0.1024430460-01    -0.2540087090-01    0.0                0.0                0.0                0.0
  0.0                 0.0                0.0                0.0                0.0                0.0
  0.0                 0.0

J = 4
  0.0                -0.5695117640-01   -0.5653720180-01   -0.5640201490-01   -0.5631033170-01   -0.5603525750-01
 -0.5564573180-01    -0.5512807870-01   -0.5446177260-01   -0.5363921740-01   -0.5262301130-01   -0.5139702400-01
 -0.4992476520-01    -0.4817156250-01   -0.4609990710-01   -0.4367425170-01   -0.4087739970-01   -0.3775054280-01
 -0.3440551490-01    -0.1160000330-01    0.0                0.0                0.0                0.0
  0.0                 0.0                0.0                0.0                0.0                0.0
  0.0                 0.0
```

```
J = 5
   0.0                  -0.564523661D-01   -0.565247137D-01   -0.564014143D-01   -0.563375011D-01   -0.560907007D-01
  -0.557J292810-01      -0.552529091D-01   -0.546J569340-01   -0.533661090D-01   -0.529291730-01    -0.518805490-01
  -0.504623433D-01      -0.480258112D0-01  -0.470471346D-01   -0.450J540210-01   -0.427660709D-01   -0.403729630D-01
  -0.380J209410-01      -0.360485807D-01    0.0                0.0                0.0                0.0
   0.0                   0.0                0.0                0.0                0.0                0.0
   0.0                   0.0

J = 6
   0.0                   0.0               -0.564873625D-01   -0.564603460D-01   -0.563428185D-01   -0.561476102D-01
  -0.558069604D-01      -0.553714315D-01   -0.548092251D-01   -0.541070951D-01   -0.532515973D-01   -0.522300317D-01
  -0.510319260D-01      -0.496611944D-01   -0.480908842D-01   -0.463684667D-01   -0.445209449D-01   -0.426643465D-01
  -0.409311603D-01       0.0                0.0                0.0                0.0                0.0
   0.0                   0.0                0.0                0.0                0.0                0.0
   0.0                   0.0

J = 7
   0.0                   0.0                0.0               -0.564071089D-01   -0.563197444D-01   -0.561394484D-01
  -0.558390040D-01      -0.554740404D-01   -0.549712609D-01   -0.543402108D-01   -0.535709376D-01   -0.526559104D-01
  -0.515971846D0-01     -0.503817017D-01   -0.490370694D-01   -0.475685787D-01   -0.460676190D-01   -0.445647249D-01
   0.0                   0.0                0.0                0.0                0.0                0.0
   0.0                   0.0                0.0                0.0                0.0                0.0
   0.0                   0.0

J = 8
   0.0                   0.0                0.0               -0.562760366D-01   -0.562610823D-01   -0.561107629D-01
  -0.558801840D0-01     -0.555505714D-01   -0.551132620D-01   -0.545532073D-01   -0.538685629D-01   -0.530534320D-01
  -0.521095610D-01      -0.510461200D-01   -0.498815923D-01   -0.486459846D-01   -0.473556076D-01   -0.460080870D-01
   0.0                   0.0                0.0                0.0                0.0                0.0
   0.0                   0.0                0.0                0.0                0.0                0.0
   0.0                   0.0

J = 9
   0.0                   0.0                0.0                0.0                0.0               -0.560583761D-01
  -0.558601305D-01      -0.555912907D-01   -0.552138892D-01   -0.547148768D-01   -0.541305661D-01   -0.534044917D-01
  -0.525625385D-01      -0.516167177D-01   -0.505911604D-01   -0.495451084D-01    0.0                0.0
   0.0                   0.0                0.0                0.0                0.0                0.0
   0.0                   0.0                0.0                0.0                0.0                0.0
   0.0                   0.0

J =10
   0.0                   0.0                0.0                0.0                0.0                0.0
  -0.557694441D-01      -0.552094783D-01   -0.545291008D-01   -0.536780641D-01   -0.526349056D-01   -0.513698075D-01
  -0.529373652D-01      -0.520762046D-01   -0.511212276D-01    0.0                0.0                0.0
   0.0                   0.0                0.0                0.0                0.0                0.0
   0.0                   0.0                0.0                0.0                0.0                0.0
   0.0                   0.0

          I          PBX2

          2          -0.564773910D-01

          3          -0.564598855D-01
```

4	-0.5627401960-01
5	-0.5619163450-01
6	-0.5539997097D-01
7	-0.5575734180-01
8	-0.5555196110-01
9	-0.5524924060-01
10	-0.5485004920-01
11	-0.5434905650-01
12	-0.5377289260-01
13	-0.5307672990-01
14	-0.5223042010-01
15	-0.5119053470-01
16	-0.4996317110-01
17	-0.4836295690-01
18	-0.4619501960-01
19	-0.4323091390-01
20	-0.3743458770-01
21	0.0
22	0.4635198490-01
23	0.9056634350-01
24	0.1346402320 00
25	0.1790518850 00
26	0.2239765310 00
27	0.2655211750 00
28	0.3157686790 00
29	0.3627854850 00
30	0.4106221210 00
31	0.4593127440 00
32	0.5088747010 00

J	PBY1	PBY2
1	-0.5650153940-01	0.5543811250 00
2	-0.5656947540-01	0.5546193820 00
3	-0.5659060000-01	-0.2303771110-01
4	-0.5655910870-01	-0.3034177930-01
5	-0.5645896630-01	-0.3571746170-01

6	0.5650556130-01	-0.3970448210-01
7	-0.5648029370-01	-0.4295116250-01
8	-0.5629420150-01	-0.4580717440-01
9	-0.5622826320-01	-0.4832529550-01
10	-0.5584911480-01	-0.5073895890-01

VELOCITY COMP. U&V IN THE X& Y DIR.

I	J	U	V
2	1	0.5406364730-03	0.0
2	2	0.4335144200-03	-0.8646499000-03
2	3	0.2759068430-03	0.1929373810-03
2	4	0.1247729110-03	0.1356382440-02
2	5	0.4809022790-03	-0.5216854200-03
3	1	0.1801589760-02	0.0
3	2	0.1068033090-02	-0.1138356640-02
3	3	0.1306875750-02	-0.3439317410-03
3	4	0.6974986610-03	0.3659768510-03
3	5	-0.2904816320-03	0.7183926420-03
3	6	0.5469169660-03	0.6482817260-03
4	1	0.3393848380-02	0.0
4	2	0.3293849940-02	-0.1359363910-02
4	3	0.2984406320-02	-0.7775970450-03
4	4	0.2486701420-02	-0.2409749470-03
4	5	0.1872125960-02	0.2166884710-03
4	6	0.1445440310-02	0.7430535850-03
4	7	0.1605493810-02	0.1835094190-02
4	8	0.2188441460-02	0.6718313070-03
5	1	0.5285266870-02	0.0
5	2	0.5200190070-02	-0.1547798690-02
5	3	0.4917703000-02	-0.1149080250-02
5	4	0.4467573750-02	-0.7463034930-03
5	5	0.3907135920-02	-0.3248684730-03
5	6	0.3327358100-02	0.1775673740-03
5	7	0.2676705390-02	0.8093616920-03
5	8	0.1580737290-02	0.1280598660-02
6	1	0.7481660090-02	0.0
6	2	0.7399268960-02	-0.1726927780-02
6	3	0.7111576540-02	-0.1510213360-02
6	4	0.6645998310-02	-0.1251542030-02
6	5	0.6045730190-02	-0.9235271810-03
6	6	0.5358580720-02	-0.4873769460-03
6	7	0.4599395980-02	0.8847337810-04
6	8	0.3800533752D-02	0.8106030540-03
6	9	0.3081247120-02	0.1550685310-02
7	1	0.1001451090-01	0.0
7	2	0.9924126330-02	-0.1917882250-02
7	3	0.9600660230-02	-0.1902350910-02
7	4	0.9071787990-02	-0.1812149840-02
7	5	0.8377915960-02	-0.1612280060-02
7	6	0.7561587420-02	-0.1266786630-02
7	7	0.6653979270-02	-0.7488815010-03
7	8	0.5681914190-02	-0.3337770460-05

7	9	0.4670873850-02	0.1124044600-02
7	10	0.4216604950-02	0.1514973860-02
8	1	0.1293830860-01	0.0
8	2	0.1282884230-01	-0.2140778440-02
8	3	0.1243793210-01	-0.2362551700-02
8	4	0.1179959200-01	-0.2474286310-02
8	5	0.1096234640-01	-0.2433727760-02
8	6	0.9977353230-02	-0.2211313630-02
8	7	0.8885438780-02	-0.1791199850-02
8	8	0.7705223540-02	-0.1172502370-02
8	9	0.6402533090-02	-0.3912685240-03
8	10	0.4783558560-02	0.9201215450-03
9	1	0.1633186330-01	0.0
9	2	0.1618952380-01	-0.2418258980-02
9	3	0.1569211900-01	-0.2931601150-02
9	4	0.1488861260-01	-0.3287735590-02
9	5	0.1384800080-01	-0.3434524870-02
9	6	0.1264356350-01	-0.3345674420-02
9	7	0.1133821640-01	-0.3021011190-02
9	8	0.9973640940-02	-0.2486243460-02
9	9	0.8564138410-02	-0.1797620360-02
9	10	0.7116341580-02	-0.4865250530-04
10	1	0.2030433640-01	0.0
10	2	0.2010937090-01	-0.2780522770-02
10	3	0.1945009810-01	-0.3663462930-02
10	4	0.1840340360-01	-0.4318404530-02
10	5	0.1707519990-01	-0.4678776860-02
10	6	0.1557627850-01	-0.4721097970-02
10	7	0.1400323310-01	-0.4461122370-02
10	8	0.1242763380-01	-0.3946580370-02
10	9	0.1089319100-01	-0.3248567880-02
10	10	0.9420318070-02	-0.1092549030-02
11	1	0.2500803450-01	0.0
11	2	0.2472957920-01	-0.3272497200-02
11	3	0.2382326040-01	-0.4637568460-02
11	4	0.2241593420-01	-0.5662633860-02
11	5	0.2067559540-01	-0.6261649940-02
11	6	0.1877063430-01	-0.6417641210-02
11	7	0.1684302470-01	-0.6169655950-02
11	8	0.1499775390-01	-0.5596285500-02
11	9	0.1330385110-01	-0.4804936070-02
11	10	0.1179988470-01	-0.2184903470-02
12	1	0.3066188400-01	0.0
12	2	0.3024881000-01	-0.3965296830-02
12	3	0.2895762340-01	-0.5977107950-02
12	4	0.2700667090-01	-0.7466069540-02
12	5	0.2466830110-01	-0.8324076700-02
12	6	0.2219671280-01	-0.8553668720-02
12	7	0.1979091550-01	-0.8234002860-02
12	8	0.1758901830-01	-0.7485753960-02
12	9	0.1568027590-01	-0.6446436980-02
12	10	0.1411691230-01	-0.3668265990-02
13	1	0.3759383630-01	0.0
13	2	0.3695670350-01	-0.4976757800-02
13	3	0.3504739800-01	-0.7879707590-02
13	4	0.3226054550-01	-0.9951956160-02
13	5	0.2904736860-01	-0.1107160800-01
13	6	0.2578687070-01	-0.1129502680-01
13	7	0.2274214610-01	-0.1077735040-01
13	8	0.2007312000-01	-0.9706925130-02
13	9	0.1787774060-01	-0.8277042060-02
13	10	0.1621871010-01	-0.5269839340-02
14	1	0.4632039500-01	0.0
14	2	0.4529269470-01	-0.6511735100-02
14	3	0.4234967570-01	-0.1067326590-01
14	4	0.3824858070-01	-0.1346609900-01

14	5	0.337520875D-01	-0.147977515D-01
14	6	0.294104184D-01	-0.148508912D-01
14	7	0.255395665D-01	-0.139477535D-01
14	8	0.222006873D-01	-0.123501595D-01
14	9	0.197137010D-01	-0.103008469D-01
14	10	0.181613741D-01	-0.693452730-02
15	1	0.577054574D-01	0.0
15	2	0.559539061D-01	-0.894747710D-02
15	3	0.511891241D-01	-0.149238215D-01
15	4	0.449731629D-01	-0.185495443D-01
15	5	0.386041052D-01	-0.199097704D-01
15	6	0.328287786D-01	-0.195075478D-01
15	7	0.279582301D-01	-0.179070815D-01
15	8	0.240013592D-01	-0.155327907D-01
15	9	0.207152926D-01	-0.123963552D-01
15	10	0.207205374D-01	-0.870611277D-02
16	1	0.733018883D-01	0.0
16	2	0.701050206D-01	-0.130280684D-01
16	3	0.619086329D-01	-0.216540091D-01
16	4	0.522250744D-01	-0.260511179D-01
16	5	0.431846371D-01	-0.269421358D-01
16	6	0.356193924D-01	-0.255047663D-01
16	7	0.297027034D-01	-0.227751729D-01
16	8	0.252598470D-01	-0.195930971D-01
16	9	0.226587295D-01	-0.147780598D-01
17	1	0.961424005D-01	0.0
17	2	0.898189811D-01	-0.203407324D-01
17	3	0.745991714D-01	-0.328037677D-01
17	4	0.592371118D-01	-0.372735402D-01
17	5	0.466243825D-01	-0.365154524D-01
17	6	0.370412024D-01	-0.329894814D-01
17	7	0.302115544D-01	-0.282666269D-01
17	8	0.263710608D-01	-0.229533791D-01
18	1	0.132606904D 00	0.0
18	2	0.1191123360 00	-0.345712974D-01
18	3	0.879701230D-01	-0.522358784D-01
18	4	0.639188479D-01	-0.540259068D-01
18	5	0.473657676D-01	-0.491380453D-01
18	6	0.359778462D-01	-0.419175944D-01
18	7	0.311645653D-01	-0.334453145D-01
18	8	0.283268629D-01	-0.266402870D-01
19	1	0.197764308D 00	0.0
19	2	0.1668382480 00	-0.650575135D-01
19	3	0.948150226D-01	-0.879972562D-01
19	4	0.615044865D-01	-0.778778956D-01
19	5	0.432438311D-01	-0.644568541D-01
19	6	0.361659276D-01	-0.519881982D-01
20	1	0.326627672D 00	0.0
20	2	0.2568578930 00	-0.137520583D 00
20	3	0.763802496D-01	-0.157569640D 00
20	4	0.505291839D-01	-0.105597098D 00
20	5	0.400380972D-01	-0.803354532D-01
21	1	0.597863976D 00	0.0
21	2	0.6219511430 00	-0.586448349D-01
22	1	0.819791237D 00	0.0
22	2	0.9056634350 00	-0.111556575D-01
23	1	0.665543077D 00	0.0
23	2	0.882882469D 00	-0.175493322D-02
24	1	0.880997851D 00	0.0
24	2	0.8946554140 00	0.258799669D-03
25	1	0.892167651D 00	0.0
25	2	0.8933631930 00	0.780437145D-03
26	1	0.9040658800 00	0.0
26	2	0.9046928970 00	0.102444196D-02
27	1	0.9174631990 00	0.0
27	2	0.9179212800 00	0.119247649D-02

28	1	0.9322822060 00	0.0
28	2	0.9326431040 00	0.1325466530-02
29	1	0.9482613520 00	0.0
29	2	0.9485344210 00	0.1429637990-02
30	1	0.9650887590 00	0.0
30	2	0.9652725850 00	0.1504911400-02
31	1	0.9824333140 00	0.0
31	2	0.9825257950 00	0.1550437610-02
32	1	0.9957920860 00	0.0
32	2	0.9958142570 00	0.1566584600-02

UBX2	VBX2
-0.6888992460-03	-0.1422398930-02
0.4121553900-03	0.5495405200-03
0.4064117160-03	0.3983631620-03
0.1871942780-02	0.1403957090-02
0.3078106240-02	0.1777145460-02
0.3358129260-02	0.1465607770-02
0.4449329330-02	0.1399249340-02
0.5130378170-02	0.1048867050-02
0.5869087620-02	0.5898655000-03
0.0	0.0
0.1567404580-01	-0.1575300880-02
0.1711227380-01	-0.3493028270-02
0.1818247250-01	-0.5718123060-02
0.1923109620-01	-0.8393138500-02
0.2192995770-01	-0.1266126700-01
0.2686264860-01	-0.2014698650-01
0.2685492370-01	-0.2632309030-01

0.3449630470-01	-0.4599507300-01
0.3740739940-01	-0.7723661400-01
0.9270396990 00	0.0
0.8842871720 00	0.0
0.8814777660 00	0.0
0.8882330630 00	0.0
0.8984933240 00	0.0
0.9108924700 00	0.0
0.9249500890 00	0.0
0.9403361190 00	0.0
0.9567327230 00	0.0
0.9738124470 00	0.0
0.9912391430 00	0.0
0.9912391430 00	0.0

UBY1	VBY1	UBY2	VBY2
-0.3166104970-04	-0.3316475060-03	0.1000000000 01	0.0
0.5591396680-04	0.3432775200-03	0.6143573590-01	-0.3009724100 00
0.1468780850-03	0.8658731940-03	0.4665675530-01	-0.1483590260 00
0.1320038620-03	0.1831403560-02	0.4009884480-01	-0.9187799570-01
0.3639753180-03	0.9548199750-03	0.3715776330-01	-0.6435913390-01
0.1463696520-02	0.1951595360-02	0.3227121570-01	-0.4302828760-01
0.3472987470-03	0.2505264290-02	0.2652376940-01	-0.2910006540-01

0.3397703590-02	0.2548277690-02	0.2439785880-01	-0.1829839410-01
0.1593413760-02	0.2150258500-02	0.2130231290-01	-0.1031718100-01

ABSOLUTE VELOCITY & ITS DIR. WITH THE X COO.

I	J	VV	THETA
2	1	0.5406364730-03	0.0
2	2	0.9672405090-03	296.6186
2	3	0.3366740540-03	34.9646
2	4	0.1362109240-02	84.7445
2	5	0.7095228530-03	312.6612
3	1	0.1801589760-02	0.0
3	2	0.2019452950-02	325.6789
3	3	0.1351374590-02	345.2464
3	4	0.7876823210-03	27.6861
3	5	0.7748984230-03	112.0397
3	6	0.8481670610-03	49.8478
4	1	0.3393848380-02	0.0
4	2	0.3563329570-02	337.5649
4	3	0.3084045760-02	345.3868
4	4	0.2500340720-02	354.4602
4	5	0.1884624520-02	6.6023
4	6	0.1625246540-02	27.2063
4	7	0.2438274190-02	48.8180
4	8	0.2289242960-02	17.0661
5	1	0.5285266870-02	0.0
5	2	0.5425648120-02	343.4155
5	3	0.5050167150-02	346.8388
5	4	0.4529479450-02	350.5071
5	5	0.3920618650-02	355.2377
5	6	0.3332092750-02	3.0548
5	7	0.2796393760-02	16.8239
5	8	0.2034370490-02	39.0120
6	1	0.7481660090-02	0.0
6	2	0.7598122180-02	346.8535
6	3	0.7270162670-02	348.0015
6	4	0.6762813830-02	349.3260
6	5	0.6115861020-02	351.3055
6	6	0.5380699170-02	354.7938
6	7	0.4600246840-02	1.1020
6	8	0.3885825860-02	12.0407
6	9	0.3994521910-02	22.8428
7	1	0.1001451090-01	0.0
7	2	0.1010774730-01	349.0529
7	3	0.9787319140-02	348.7829
7	4	0.9251012080-02	348.6942
7	5	0.8531643560-02	349.0976
7	6	0.7667292450-02	350.4657

7	7	0.6695988620-02	353.5693
7	8	0.5681915170-02	359.9571
7	9	0.4804220930-02	13.5310
7	10	0.4480502550-02	19.7628
8	1	0.1293830680-01	0.0
8	2	0.1300623410-01	350.5169
8	3	0.1266032410-01	349.2357
8	4	0.1205622100-01	348.1478
8	5	0.1122925060-01	347.4736
8	6	0.1021946600-01	347.4941
8	7	0.9064183320-02	348.5933
8	8	0.7793922730-02	351.3384
8	9	0.6414477460-02	356.4937
8	10	0.4871247900-02	10.8880
9	1	0.1633186330-01	0.0
9	2	0.1636913730-01	351.4952
9	3	0.1596361120-01	349.4087
9	4	0.1524729450-01	347.5384
9	5	0.1426755360-01	346.0615
9	6	0.1307873210-01	345.1691
9	7	0.1173378290-01	345.0712
9	8	0.1027885790-01	345.9932
9	9	0.8750766010-02	348.1364
9	10	0.7116507890-02	359.5991
10	1	0.2030433640-01	0.0
10	2	0.2030069220-01	352.1184
10	3	0.1979210140-01	349.3239
10	4	0.1890327700-01	346.7850
10	5	0.1770461530-01	344.6672
10	6	0.1627603200-01	343.1289
10	7	0.1469667140-01	342.3200
10	8	0.1303923220-01	342.3727
10	9	0.1136726900-01	343.3851
10	10	0.9483462230-02	353.3753
11	1	0.2500803450-01	0.0
11	2	0.2494516640-01	352.4525
11	3	0.2427045070-01	348.9750
11	4	0.2312011090-01	345.8135
11	5	0.2160297440-01	343.1417
11	6	0.1983740990-01	341.1152
11	7	0.1793745060-01	339.8727
11	8	0.1600784280-01	339.5281
11	9	0.1414495900-01	340.1326
11	10	0.1200046180-01	349.5005
12	1	0.3066188400-01	0.0
12	2	0.3050760700-01	352.5225
12	3	0.2956805330-01	348.3282
12	4	0.2801968000-01	344.5371
12	5	0.2603488690-01	341.3442
12	6	0.2378779740-01	338.9161
12	7	0.2143546460-01	337.4009
12	8	0.1911570240-01	336.9364
12	9	0.1695368990-01	337.6423
12	10	0.1458572550-01	345.4246
13	1	0.3759383630-01	0.0
13	2	0.3729029430-01	352.3212
13	3	0.3592227580-01	347.3196
13	4	0.3376069060-01	342.8464
13	5	0.3108585090-01	339.1260
13	6	0.2815209280-01	336.3366
13	7	0.2516657490-01	334.6347
13	8	0.2229696260-01	334.1833
13	9	0.1970083840-01	335.1475
13	10	0.1705337990-01	341.9905
14	1	0.4632039500-01	0.0
14	2	0.4575839690-01	351.8094

14	3	0.4367394690-01	345.8452
14	4	0.4054984280-01	340.5952
14	5	0.3685345110-01	336.3168
14	6	0.3295086280-01	333.1866
14	7	0.2909998780-01	331.3507
14	8	0.2547460430-01	330.9911
14	9	0.2224269440-01	332.4026
14	10	0.1944025540-01	339.0923
15	1	0.5770545740-01	0.0
15	2	0.5666477700-01	350.9056
15	3	0.5332022950-01	343.7370
15	4	0.4864844270-01	337.5766
15	5	0.4343588250-01	332.7086
15	6	0.3818734250-01	329.2710
15	7	0.3320129810-01	327.3513
15	8	0.2858903340-01	327.0812
15	9	0.2414110540-01	329.0937
15	10	0.2247525460-01	337.2001
16	1	0.7330188830-01	0.0
16	2	0.7130529070-01	349.4632
16	3	0.6558639290-01	340.7122
16	4	0.5836196660-01	333.4795
16	5	0.5089981890-01	328.0313
16	6	0.4380906550-01	324.3866
16	7	0.3742938810-01	322.5107
16	8	0.3196794210-01	322.1913
16	9	0.2705196990-01	326.8782
17	1	0.9614240050-01	0.0
17	2	0.9209340240-01	347.2305
17	3	0.8149308900-01	336.2540
17	4	0.6998822910-01	327.8115
17	5	0.5922171310-01	321.9232
17	6	0.4960198140-01	318.3018
17	7	0.4137318240-01	316.8955
17	8	0.3496127080-01	318.9543
18	1	0.1326869040 00	0.0
18	2	0.1240279130 00	343.8058
18	3	0.1023099680 00	329.2892
18	4	0.8369239940-01	319.7852
18	5	0.6825000680-01	313.9385
18	6	0.5524029450-01	310.6301
18	7	0.4571454020-01	312.9689
18	8	0.3888593640-01	316.7481
19	1	0.1977643080 00	0.0
19	2	0.1790739540 00	338.6877
19	3	0.1293576650 00	317.1264
19	4	0.9923592330-01	308.2907
19	5	0.7761870520-01	303.8482
19	6	0.6333045930-01	304.8152
20	1	0.3266276720 00	0.0
20	2	0.2913552600 00	331.8263
20	3	0.1751060650 00	295.8518
20	4	0.1170638530 00	295.5621
20	5	0.8975987010-01	296.4816
21	1	0.5978639760 00	0.0
21	2	0.6247098850 00	354.6042
22	1	0.8190912370 00	0.0
22	2	0.9057321380 00	359.2851
23	1	0.8655430770 00	0.0
23	2	0.8828842120 00	359.8769
24	1	0.8809978510 00	0.0
24	2	0.8848554460 00	0.0155
25	1	0.8921676510 00	0.0
25	2	0.8933635340 00	0.0501
26	1	0.9040658800 00	0.0
26	2	0.9046934770 00	0.0649

27	1	0.9174631990 00	0.0
27	2	0.9179220540 00	0.0744
28	1	0.9322822060 00	0.0
28	2	0.9326440460 00	0.0814
29	1	0.9482613520 00	0.0
29	2	0.9485354980 00	0.0864
30	1	0.9650887590 00	0.0
30	2	0.9652737580 00	0.0893
31	1	0.9824333140 00	0.0
31	2	0.9825270180 00	0.0904
32	1	0.9957920860 00	0.0
32	2	0.9958154880 00	0.0901

I	J	VVBX	THETA
2	1	0.0	0.0
2	2	0.1580443260-02	244.1823
3	1	0.0	0.0
3	2	0.6869256500-03	53.1303
4	1	0.0	0.0
4	2	0.5690902310-03	44.4272
5	1	0.0	0.0
5	2	0.2339928480-02	36.8700
6	1	0.0	0.0
6	2	0.3554290930-02	30.0001
7	1	0.0	0.0
7	2	0.3664019420-02	23.5783
8	1	0.0	0.0
8	2	0.4664164470-02	17.4577
9	1	0.0	0.0
9	2	0.5244335260-02	11.5370
10	1	0.0	0.0
10	2	0.5898655000-02	5.7392
11	1	0.2756495030-01	0.0
11	2	0.0	0.0
12	1	0.3375881780-01	0.0
12	2	0.1575300880-01	354.2516
13	1	0.4142885480-01	0.0
13	2	0.1746514130-01	348.4538
14	1	0.5121193510-01	0.0
14	2	0.1906041020-01	342.5331
15	1	0.6419897970-01	0.0
15	2	0.2098284620-01	336.4125
16	1	0.8240479690-01	0.0
16	2	0.2532253390-01	329.9907
17	1	0.1098800040 00	0.0
17	2	0.3357831080-01	323.1207
18	1	0.1554938040 00	0.0
18	2	0.3760441480-01	315.5636
19	1	0.2400348120 00	0.0
19	2	0.5749384120-01	306.8605
20	1	0.4132205330 00	0.0
20	2	0.8581846000-01	295.8325
21	1	0.7825074200 00	0.0
21	2	0.9270396990 00	0.0
22	1	0.8556750550 00	0.0
22	2	0.8842871720 00	0.0
23	1	0.8754111000 00	0.0
23	2	0.8814777060 00	0.0
24	1	0.8865846010 00	0.0
24	2	0.8882330630 00	0.0
25	1	0.8977507000 00	0.0
25	2	0.8984933240 00	0.0
26	1	0.9103810600 00	0.0
26	2	0.9108924700 00	0.0

27	1	0.9245453370 00	0.0
27	2	0.9249500890 00	0.0
28	1	0.9400190750 00	0.0
28	2	0.9403361190 00	0.0
29	1	0.9566036300 00	0.0
29	2	0.9567327230 00	0.0
30	1	0.9736738890 00	0.0
30	2	0.9738124470 00	0.0
31	1	0.9911927390 00	0.0
31	2	0.9912391430 00	0.0
32	1	0.9911927390 00	0.0
32	2	0.9912391430 00	0.0

I	J	VVBY	THETA
1	2	0.3331553550-03	264.5711
2	2	0.1000000000 01	0.0
1	3	0.3478014190-03	80.7491
2	3	0.3071786790 00	281.5274
1	4	0.8782424470-03	80.3728
2	4	0.1555225180 00	287.4481
1	5	0.1836154690-02	85.8777
2	5	0.1002471120 00	293.5687
1	6	0.1021841090-02	69.1335
2	6	0.7431552660-01	299.9905
1	7	0.2439494200-02	53.1303
2	7	0.5378535950-01	306.8605
1	8	0.2529222330-02	82.1078
2	8	0.4074824200-01	314.4176
1	9	0.4247129490-02	36.8700
2	9	0.3049732360-01	323.1207
1	10	0.2676299510-02	53.4605
2	10	0.2366923600-01	334.1487